HHS Public Access

Author manuscript

Neuron. Author manuscript; available in PMC 2024 November 01.

Published in final edited form as:

Neuron. 2023 November 01; 111(21): 3479–3495.e6. doi:10.1016/j.neuron.2023.08.007.

Differential Cortical Network Engagement During States of Un/Consciousness in Humans

Rina Zelmann[1,2], **Angelique C. Paulk**[1,2], **Fangyun Tian**[3], **Gustavo A. Balanza Villegas**[3], **Jaquelin Dezha Peralta**[1], **Britni Crocker**[1,4], **G. Rees Cosgrove**[5], **R. Mark Richardson**[6], **Ziv M. Williams**[6], **Darin D. Dougherty**[7], **Patrick L. Purdon**[3], **Sydney S. Cash**[1,2]

[1]Department of Neurology, Massachusetts General Hospital, Boston, MA, USA

[2]Center for Neurotechnology and Neurorecovery, Massachusetts General Hospital, Boston, MA, USA.

[3]Department of Anesthesia, Massachusetts General Hospital, Boston, MA, USA

[4]Harvard-MIT Health Sciences and Technology, Institute for Medical Engineering and Science, Massachusetts Institute of Technology, Cambridge, MA, 02139

[5]Department of Neurosurgery, Brigham and Women's Hospital, Boston, MA, USA

[6]Department of Neurosurgery, Massachusetts General Hospital, Boston, MA, USA

[7]Department of Psychiatry, Massachusetts General Hospital, Boston, MA, USA

Summary

What happens in the human brain when we are unconscious? Despite substantial work, we are still unsure which brain regions are involved and how they are impacted when consciousness is disrupted. Using intracranial recordings and direct electrical stimulation, we mapped global, network, and regional involvement during wake vs. arousable unconsciousness (sleep) vs. non-arousable unconsciousness (propofol-induced general anesthesia). Information integration and complex processing were reduced, while variability increased in any type of unconscious state. These changes were more pronounced during anesthesia than sleep and involved different cortical engagement. During sleep, changes were mostly uniformly distributed across the brain

Corresponding author and lead contact: Rina Zelmann, rzelmann@mgh.harvard.edu.

Author contributions

Conceptualization, R.Z., D.D.D., and S.S.C.; Methodology, R.Z. and S.S.C.; Software, R.Z., B.C., and A.C.P.; Investigation, R.Z., A.C.P., F.T., G.A.B.V., J.D.P., B.C., G.R.C, R.M.R, Z.M.W., and S.S.C.; Resources, G.R.C., R.M.R., Z.M.W., P.L.P., and S.S.C; Data Curation, R.Z., J.D.P, and A.C.P; Writing – Original Draft, R.Z. and S.S.C.; Supervision, S.S.C.; Funding Acquisition, R.Z., D.D.D, and S.S.C.

Declaration of interests

P.L.P is a co-founder of PASCALL Systems, Inc., a company developing closed-loop physiological control systems for anesthesiology. D.D.D. receives consulting fees from Sage and Celanese, has equity from Innercosmos and Neurable, and receives research support from Medtronic. S.S.C. is an advisor to Beacon Biosignals.

P.L.P. is an inventor on patents assigned to MGH related to brain monitoring, an inventor on a patent licensed to Masimo by MGH. D.D.D. is an inventor on patents related to mental and emotional disorders and neuro-stimulation.

All the other authors declare no competing interests.

while during anesthesia the prefrontal cortex was the most disrupted, suggesting that the lack of arousability during anesthesia results not from just altered overall physiology but from a disconnection between prefrontal and other brain areas. These findings provide direct evidence for different neural dynamics during loss of consciousness compared to loss of arousability.

eTOC Blurb

What happens in the human brain when we are unconscious? Zelmann et al., provide direct experimental evidence that during unconsciousness, such as natural sleep, the human brain is uniformly affected, while lack of arousability during general anesthesia, is linked to a profound disruption of function and connectivity in prefrontal regions.

Graphical Abstract:

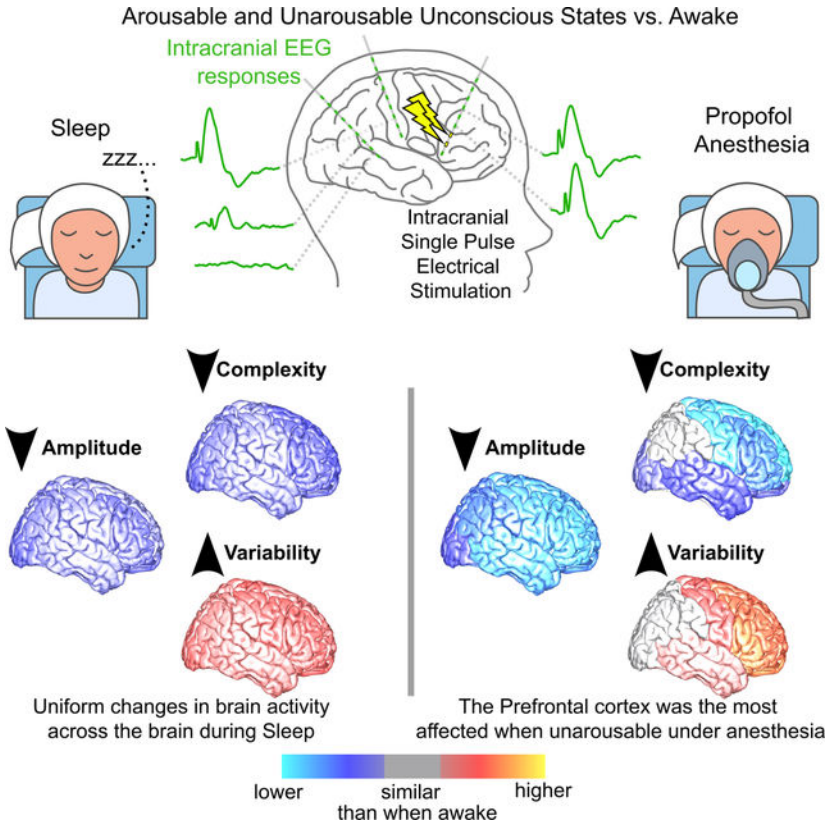

Keywords

Consciousness; Cortico-cortical evoked potential; Intracranial EEG; Propofol-induced general anesthesia; Sleep; Complexity reduction; Connectivity reduction; Variability Increase; Prefrontal cortex; Lack of arousability during anesthesia

Introduction

Understanding the neuronal mechanisms underlying consciousness is one of the greatest challenges in human neuroscience. Despite decades of research, there are more controversies

than agreements. One of the most powerful ways to study consciousness and arousability is to compare the intra-individual physiology of the conscious awake state with two of the most obvious non-pathological unconscious states: natural sleep and general anesthesia. Dissecting similarities and differences between these uniquely defined states at the neural network level and the corresponding regional involvement in the human brain is paramount to obtaining a deeper understanding of consciousness and arousability.

Theories of consciousness[1–8] and experimental studies[9–11] differ concerning which brain regions are necessary for consciousness and arousability. In particular, the role of the prefrontal cortex (PFC) is at the center of avid debate[12,13]. Direct experimental evidence to resolve this debate requires identifying the global, network, and regional involvement during wake vs. arousable unconsciousness (e.g., non-rapid eye-movement [non-REM] sleep) vs. non-arousable unconsciousness (e.g., propofol-induced general anesthesia). Despite both being states of unconsciousness and being similar in some physiological parameters, they have important differences[14–16]. What non-REM sleep and anesthesia have in common is loss of consciousness and what distinguishes them is the fact that the unconsciousness of sleep can be reversed by stimuli of sufficient strength. One challenge is understanding whether anesthesia is amplified sleep (a “deep sleep”) or if different neuronal mechanisms are involved. If the former, similar neural networks should be disrupted under both anesthesia and sleep, albeit to a different degree. If the latter, cortical regions would be differentially altered between the two states.

A robust approach for understanding brain networks and their sensitivity to state is to examine responses to perturbations. This can be done safely and in a controlled fashion using direct electrical stimulation. Moreover, as brain stimulation is increasingly used as a chronic therapeutic approach in neurological[17–23] and neuropsychiatric disorders[24–27], understanding the brain’s response to stimulation during different brain states is important in its own right. Since Penfield’s seminal mapping of the homunculus[28], stimulation with simultaneous intracranial EEG recordings has become invaluable as a research and clinical tool. Brief single pulses of electrical stimulation (SPES[29]) produce consistent cortico-cortical evoked potentials (CCEP[30,31]). CCEP connectivity measures the way the response to stimulation spreads[32], likely a combination of anatomical and functional networks[33], revealing human brain connections[34,35], epileptic networks[36–39], and allowing intraoperative language mapping[40].

Studies to date aimed at differentiating consciousness from altered consciousness states[41–44], implicitly focusing on common characteristics across unconscious states during spontaneous activity[41] or following perturbations[44–48]. Interestingly, details of those studies suggest potential differences across types of loss of consciousness. Taking this into account as well as the general theories of consciousness[1–6,8,49] and animal stimulation studies[9,10,50,51] we hypothesize that the brain’s response to SPES perturbations is different while awake, during natural sleep, and under propofol-induced general anesthesia. We also hypothesize that the differences between arousable vs. non-arousable unconsciousness are region specific. Specifically, we hypothesize that the PFC will be less responsive to SPES during anesthesia than during sleep, while posterior regions will be similarly affected regardless of the cause of loss of consciousness (LOC).

Here we examined human neural reactivity with SPES while recording via intracranial electrodes to infer the global, network, and intrinsic neural correlates of un/consciousness and arousability. We used perturbational complexity as a summary of functional integration and differentiation in the brain's response to stimulation[42,52,53]. CCEP connectivity, sometimes referred to as effective connectivity[32,36], was measured as a reflection of information transfer[35,36]. Intrinsic characteristics were measured by the amplitude of the responses and inter-stimulation variability, a measure of underlying stability[54–56]. Complexity and connectivity measures were reduced while variability increased during both unconscious states, compared to wake. During sleep, changes were mostly homogenous across brain regions. In contrast, during anesthesia, the PFC was the most disrupted. These results provide direct evidence of increased variability in the neural responses, reduced information transfer, and reduced complexity during LOC from human intracranial recordings. However, these metrics differ depending on arousable (sleep) vs. unarousable (anesthesia) LOC as well as brain regions examined.

Results

Pseudo-random multi-region intracranial SPES (at seven mA, biphasic, bipolar, charge-balanced, duration 233 μsec) was delivered while simultaneously recording intracranial EEG (iEEG) in 20 patients with semi-chronic depth-electrodes implanted for clinical reasons to localize the focus of their seizures (median age= 37.5, range: [18 61]; 10 women). SPES was delivered in the epilepsy monitoring unit (EMU) while participants were awake (N=17) or during non-REM sleep, stages N2 or N3, at the beginning of the night (N=13) and during the electrode explantation procedure in the operating room (OR) while awake (N=16) and following propofol-induced general anesthesia (N=14). Awake in the EMU or the OR corresponded to conscious states under different environments; a normalizing element to allow a direct comparison of sleep vs. anesthesia.

Only contacts outside the clinically determined epileptic network were included. After excluding stimulation channels that did not evoke CCEPs (see "Methods - Channel selection"), a total of s=115 stimulation channels (median: 5 range: [1 14] per participant) and r=2357 bipolar recording channels (120 [29 177] per participant) were included across the 20 participants (Table S1; distribution in Fig. 1.a & S1). Brain's responses were compared while awake vs. sleep in the EMU (N=13, s=99, r=1547; Fig. S1.c), awake vs. anesthesia in the OR (N=14, s=36, r=1709; Fig. S1.d), and awake in different environments (N=13, s=34, r=1479). In seven participants, SPES was delivered during all four states (s=20; r= 899).

1. Brain responses decreased and variability increased during unconsciousness.

Conscious (awake) and unconscious states (sleep and anesthesia) were compared with different measures of complex network dynamics: perturbational complexity[43], CCEP network connectivity[30,57], CCEP response features, and response variability. We chose these measures as they are widely employed in neuroscience in general and consciousness research in particular and are highly representative of network and local circuit level

responses which we hypothesized would be differentially altered in specific states of consciousness.

Overall functional information integration and differentiation, was estimated with the perturbation complexity index (PCI)[58]. PCIst, based on principal components analysis (PCA), is the adaption of PCI for intracranial or sparse recordings[52]. PCIst was reduced during sleep compared to awake ($p<<0.001$, $m_{Awake}=56.1$, $m_{Sleep}=35.8$, $s=99$; Wilcoxon test; Table S2; Fig 2.a & 2.c) in participants whose recordings were acquired in the EMU. The same was true, in the OR, for anesthesia compared to awake ($p<<0.001$, $m_{Awake}=60.9$, $m_{Anesthesia}=28.5$, $s=36$). At a per participant level, the maximum PCIst value, corresponding to the stimulation site producing the most complex response per participant and state[59], was higher in wakefulness than either sleep ($p=0.0002$, $m_{Awake}=82.5$, $m_{Sleep}=50.4$, $N=13$) or anesthesia ($p=0.0001$, $m_{Awake}=65.5$, $m_{Anesthesia}=29.6$, $N=14$; Wilcoxon test; Fig. 2.c) for each participant (Fig. S2.a).

To understand how stimulation connectivity, which represents network information transfer[32], was affected by state, causal network centrality measures were implemented. Casual indegree centrality or CCEP connectivity is essentially the percentage of recording channels with CCEP responses during each state (Fig. 1.b–e). For each stimulation site, channels with CCEP responses were channels with peak amplitude or area under the curve larger than a null distribution created from baseline segments (see “Methods – CCEP connectivity” for details). Compared to wakefulness in the corresponding environment, CCEP connectivity was reduced during sleep ($p<<0.0001$, $m_{Awake}=9\%$, $m_{Sleep}=6\%$, $s=99$, Wilcoxon test) and during anesthesia ($p<<0.0001$, $m_{Awake}=8\%$, $m_{Anesthesia}=1.5\%$, $s=36$; Table S2; Fig 2.d). The causal outdegree centrality measure, essentially the percentage of stimulations that produced a response per recording channel[32,60], was also smaller for unconscious compared to conscious states. Casual outdegree was reduced during sleep ($p<<0.0001$, $m_{Awake}=15\%$, $m_{Sleep}=11\%$, $r=860$, Wilcoxon test) and during anesthesia ($p<<0.0001$, $m_{Awake}=25\%$, $m_{Anesthesia}=0\%$, $r=562$; Table S2; Fig 2.d). At a per-participant level, the network density, the number of connections divided by the number of possible connections[32,60], was higher in wakefulness than either sleep ($p=0.03$, $N=13$) or anesthesia ($p=0.0001$, $N=14$; Wilcoxon test; Fig. S2.b).

These differences in perturbational complexity and connectivity measures suggest that overall complex neural processing was disrupted during unconsciousness, both sleep and anesthesia.

The finest level of detail corresponded to intrinsic characteristics, measured as features of the responses. A linear mixed-effect model (LMM) was implemented to analyze the effect of state in features, controlling for the number of trials and brain location of recordings and stimulation, with participants as the random effect. The amplitude of the responses, measured as the maximum-minimum z-scored amplitude following stimulation, was smaller for unconscious compared to conscious states. The LMM model showed a significant effect of state on amplitude ($p<<0.001$), but no significant effect was observed for the number of trials ($p=0.9$), recording ($p=0.9$), or stimulation location ($p=0.8$; Table S3). In pairwise comparisons, there were significant differences comparing awake to sleep

($p<<0.001$, $m_{Awake}=6.0$, $m_{Sleep}=3.8$; $r=1527$; permutation test) or to anesthesia ($p<<0.001$, $m_{Awake}=5.5$, $m_{Anesthesia}=1.7$, $r=573$; Table S3; Fig 2.e). During anesthesia, this reduction was systematic, with 96% of the recording channels showing a reduction in amplitude. During sleep, the amplitude was reduced in 82% of the channels (Fig. 1.c & 2.a), while in 18% it was similar (Fig. 2.b) or even larger during sleep than awake (Fig. S3).

The variability of the responses following stimulation was measured as the standard deviation for individual trials, averaged across trials (Fig. 2.b). Overall, response variability was larger for unconscious compared to conscious states. The LMM showed that state ($p<<0.001$) but not number of trials ($p=0.4$), recording ($p=0.1$), or stimulation location ($p=0.8$) had a significant effect on variability (Table S3). In pairwise comparisons, variability was significantly higher while asleep than awake ($p << 0.001$, $m_{Awake} = 1.4$, $m_{Sleep} = 1.7$; $r = 1527$; permutation test) and under anesthesia than awake ($p << 0.001$, $m_{Awake} = 1.4$, $m_{Anesthesia} = 1.8$, $r = 573$; Fig. 2.f; Table S3).

To ensure that overall complex dynamics and connections were similar in the different environments, we compared awake in the EMU and the OR ($N = 13$; $s = 34$; $r = 642$). There was no significant difference between awake in different environments for complexity, connectivity, or variability measures and a significant difference for amplitude (Table S2 & S3; Fig. 2). To control for this and other heterogeneities, relative measures normalized by awake in each environment were used in the following sections.

2. Brain responses are more disrupted during anesthesia than during sleep.

The preceding comparisons focused on the physiology of conscious vs. both unconscious states. We now compare arousable (sleep) and unarousable (under anesthesia) states of unconsciousness. To allow a direct comparison between sleep and anesthesia, relative measures were computed by normalizing them to their corresponding wake state (see “Methods – Relative measures” for details). These normalized measures, bounded between −1 and +1 with zero representing no difference between states, controlled for heterogeneities due to patient etiologies, electrode location, recording environments, head position, medication levels, and other parameters.

Across measures, the median relative values of wake states, corresponding to the difference between wake in different environments, was zero, indicating similar overall complexity, connectivity, and variability (Fig 3). However, the dispersion was large, emphasizing the importance of using normalized measures to compare sleep and anesthesia.

The relative perturbational complexity for sleep and for anesthesia compared to awake in the same participant and environment was negative for most stimulated channels (Fig 3.a), in line with complexity reduction during unconscious states (Fig 2.c). Overall, relative complexity in anesthesia was significantly lower than during sleep ($p=0.001$, $m_{RelSleep}=-0.24$, $m_{RelAnesth}=-0.37$, $s_{Sleep}=99$, $s_{Anesth}=36$, Mann-Whitney U-test; Table S4; Fig 3.a).

The relative CCEP connectivity and the outdegree were also mainly negative for sleep and anesthesia, indicating fewer connections when not awake (Fig. 3.b & c), in line

with CCEP connectivity decrease during unconscious states (Fig. 2.d). Again, these measures of relative connectivity were not equivalent for both unconscious states. The relative CCEP indegree connectivity was significantly smaller for anesthesia than for sleep ($p<<0.001$, $m_{RelSleep}=-0.18$, $m_{RelAnesth}=-0.74$, $s_{Sleep}=99$, $s_{Anest}=36$, Mann-Whitney U-test; Table S4; Fig. 3.b). This difference remained if considering stimulation primarily in white matter tracks or in gray matter (Table S4). The relative outdegree was significantly smaller for anesthesia than for sleep ($p<<0.001$, $m_{RelSleep}=0$, $m_{RelAnest}=-1$; $r_{RelSleep}=860$, $r_{RelAnest}=562$; Mann-Whitney U-test; Table S4; Fig. 3.c).

Intrinsic characteristics might help in understanding this decrease in connectivity. When analyzing relative CCEP features, the median relative amplitude for sleep and anesthesia was negative (Fig. 3.d), indicating diminished CCEP responses, in line with decreased connections and amplitude during unconsciousness (Fig 2.e). An LMM with relative amplitude as the dependent variable and with fixed and random effects as before, showed that being asleep or under anesthesia ($p<<0.001$), but not the number of trials ($p=0.4$), recording ($p=0.4$), or stimulation location ($p=0.7$) had a significant effect on amplitude (Table S5). Unpaired comparisons also showed that the relative amplitude was significantly smaller for anesthesia than sleep ($p<<0.001$, $m_{RelSleep}=-0.26$, $m_{RelAnest}=-0.49$; $r_{RelSleep}=1527$, $r_{RelAnest}=573$; permutation test; Fig. 3.d; Table S5). As an additional step, to reduce potential biases towards more stable states only channels with responses in both states were compared. The peak-to-peak amplitude of the detected peaks and the latency of the first peak of the CCEP responses were computed. Also in this more restricted case, the LMM model showed that the amplitude of the responses depended on state ($p<<0.001$) but not on number of trials ($p=0.5$), recording ($p=0.8$), or stimulation location ($p=0.4$; Table S5). The relative peak-to-peak amplitude of the CCEP responses was significantly smaller for anesthesia than sleep ($p<<0.001$, $m_{RelSleep}=-0.21$, $m_{RelAnest}=-0.34$; $r_{RelSleep}=732$, $r_{RelAnest}=84$; permutation test; Fig. 3.e; Table S5). There was no effect of state in the latency of the first peak (Table S5).

The relative variability was mostly positive for anesthesia and sleep (Fig. 3.f), in line with the variability increase during unconsciousness (Fig. 2.f). The LMM model showed that variability depended on being asleep or under anesthesia ($p<<0.001$; Table S5) as well as on recording location ($p<<0.001$), but not on the number of trials ($p=0.5$) or stimulation location ($p=0.2$). Variability was significantly larger for anesthesia than for sleep ($p<<0.001$; $m_{RelSleep}=0.26$, $m_{RelAnest}=0.38$; $r_{Sleep}=1527$, $r_{Anest}=573$; permutation test; Fig. 3.f; Table S5).

Together, these relative measures allowed a direct comparison of arousable vs. unarousable states of unconsciousness. These results suggest that although there was loss of information in any form of unconsciousness, this was more profound with anesthesia than with sleep. However, there was more variance in the aggregate responses than expected, and the LMM models suggested an effect of recording channel location on the variability. Therefore, we studied the interaction between regions and relative measures.

3. The anatomical distribution differs between sleep and anesthesia.

To understand whether decreased complexity, connectivity, and response amplitude, as well as increased variability, were uniformly distributed across the brain or if they were defined anatomically, these relative measures were visualized on a template brain[61,62]. Anatomical regions were parcellated in each participant's native space, relative measures averaged for each sub-lobular region, and plotted on a stereotactic brain surface.

Complexity was uniformly reduced across brain regions for sleep but not for anesthesia. In anesthesia, the frontal and temporal lobes were especially affected (Fig. 3.a). In terms of connectivity measures, there was a greater reduction of relative CCEP indegree connectivity during anesthesia than during sleep across the brain. This reduced CCEP connectivity during anesthesia was more pronounced for stimulation in frontal and temporal channels than for posterior channels (Fig 3.b). When analyzing each individual stimulation, these regional differences can be appreciated from individual channels (Fig. S4). The relative outdegree centrality was uniformly reduced during sleep and further reduced during anesthesia, with a more pronounced reduction in anterior than posterior cortices (Fig 3.c).

The relative amplitude of the responses was also uniformly reduced during sleep. During anesthesia, there was a more substantial reduction in frontal regions than in any other region (Fig. 3.d & e). This occurred whether all responsive channels were considered (Fig. 3.d) or even when the amplitude was computed on the detected CCEP responses (Fig 3.e), which were uncommon during anesthesia.

Relative variability uniformly increased across brain regions during sleep. However, during anesthesia, there was an apparent dichotomy between anterior and posterior or temporal regions, with a marked increase in variability in the PFC. In contrast, less increase was observed in posterior or temporal regions than during sleep (Fig. 3.f).

As an alternative view, the subtraction of these relative measures between anesthesia and sleep further illustrates the differential involvement of frontal and posterior regions (Fig. 3.g), suggesting a disconnection of frontal regions related to lack of arousability during anesthesia.

4. The PFC was particularly affected during anesthesia.

Not all brain regions were altered by the different states of consciousness equally. The PFC was particularly interesting as all the measures differentiated anesthesia from sleep (Fig. 3 & 4). The PFC (including lateral and orbitofrontal cortices) was statistically compared to *posterior* (posterior cingulate, parietal, lingual, and occipital cortices) and *temporal* (amygdala, hippocampus, fusiform, and temporal) regions.

During sleep, activity across brain regions was predominately uniformly altered (Fig. 3). Indeed, complexity, indegree, and amplitude decreased, while variability increased during sleep compared to awake irrespective of where in the brain stimulation was delivered (Table S2) or signals recorded (Table S3). Outdegree during sleep was slightly different; it was significantly smaller for prefrontal and temporal but not for posterior regions (Table S2). No significant difference was found when stimulation was delivered to the PFC compared to

posterior or temporal regions, for relative complexity and indegree (Table S6; Fig. 5.a&b). There was a statistically significant difference for outdegree, amplitude across channels, and variability, while no statistical difference was found when only considering detected CCEP responses (Table S6; Fig. 5.c–f). Thus, in line with the observed uniform distribution across the brain during sleep (Fig. 3), there were small differences across regions, individual stimulations (Fig. S4), and measures, but with overall homogenous disengagement during sleep.

In contrast, during anesthesia, the PFC was exceptionally affected (Fig. 4). Perturbational complexity and indegree connectivity decreased irrespective of where stimulation was delivered (Table S2), but the decrease was significantly more for PFC than posterior stimulation (Table S6; Fig. 5.a&b). At the recording channel level, outdegree and amplitude were significantly reduced irrespective of recording region (Table S3), with relative measures significantly lower in the PFC than in posterior regions (Table S6; Fig 5.c–e). Similarly, inter-stimulation variability was significantly larger when comparing anesthesia vs. awake irrespective of recording region (Table S3), with relative variability higher in the PFC than in posterior or temporal regions (Table S6; Fig. 5.f).

Most importantly, when directly comparing sleep and anesthesia with normalized measures, the relative complexity was lower for anesthesia than sleep for PFC ($p=0.02$, U-Mann test, Table S4; Fig. 5.a) but not for posterior stimulation ($p=0.5$). The relative indegree, outdegree, and amplitude were significantly lower for anesthesia than sleep for each stimulated or recording region, but it was the lowest for the PFC (Tables S4&5; Fig. 5.b–d). The relative amplitude of those detected CCEPs was significantly smaller during anesthesia than sleep only in the PFC ($p<<0.001$, permutation test, Table S5; Fig. 5.e). Interestingly, the relative variability was higher during anesthesia than sleep when recording in PFC ($p<<0.001$, permutation test, Table S5; Fig. 5.f) while the opposite was observed for posterior and temporal channels, for which the relative variability was lower during anesthesia than sleep (posterior: $p<<0.001$, temporal: $p=0.02$). Thus, the PFC was specifically disconnected during anesthesia, but not during sleep. For all these measures, when subdividing the PFC in dorsolateral (dlPFC), ventrolateral (vlPFC), dorsomedial (dmPFC), and orbitofrontal (OF) subregions, these differences hold for each subregion (Table S5; Fig. 6).

Discussion

We studied the electrophysiological response of the human brain to stimulation during conscious, arousable unconscious (non-REM sleep), and unarousable unconscious (propofol-induced general anesthesia) states with 1) global measures of functional integration and differentiation (Perturbational complexity), 2) network measures of information transfer (CCEP connectivity and CCEP features), and 3) a measure of response stability (inter-trial variability). Overall complexity and connectivity decreased when consciousness was lost, responses were fewer and smaller, and variability was larger. However, these results were not identical for different states of unconsciousness. Relative measures showed that these differences were more pronounced during anesthesia than sleep, with a relative increase in response variability and a decrease in information transfer

capabilities during anesthesia. This aligns with behavioral and physiological differences between sleep and propofol-induced anesthesia[14,15,63,64]. Finally, informed by the brain-wide distribution of the measures, that suggested different anatomical distributions during sleep and anesthesia, prefrontal, posterior, and temporal regions were contrasted. Relative complexity and connectivity measures were similarly reduced in posterior regions during sleep or anesthesia, but during anesthesia, the reduction was significantly more pronounced in the PFC. Correspondingly, variability increased uniformly during sleep, but during anesthesia, variability was higher in the PFC. Together our results suggest a distinct response to stimulation for different states and brain regions, with the PFC particularly affected by anesthetic drugs.

The regional differences during anesthesia suggest that lack of arousability may be related to the overall reduction of information integration with loss of effective connections in anterior areas. Sleep showed a more homogenous disengagement and one of lesser magnitude. The overall uniform changes during sleep suggest that even though sleep oscillations are, to some extent, local phenomena[65–68], the response to perturbations across the brain is similar. This might correspond to thalamocortical synchronization during sleep[69–71]. In contrast, the disruption of PFC functional measures during anesthesia, also manifested by the disappearance of correlation between complexity and connectivity (Fig. S5.a), may reflect an overall difference in suppression of background synaptic activity. Propofol-induced general anesthesia likely produces deeper metabolic suppression than sleep[14], comparable to that seen in coma from anoxic encephalopathies or structural brain injuries[72]. As a plausible explanation, the ‘mesocircuit’ hypothesis[8] suggested that the selective impact of the PFC as graded by a reduction in overall background activity may reflect not only corticothalamic disruption but also shutdown of the fronto-striatal-pallidal-thalamic loop activity[8,73]. In line with this, studies of spontaneous electrophysiology suggested that propofol disrupts thalamocortical connections[74–79] by enhancing $GABA_A$ inhibition[63,80], imposing a unique rhythm predominantly observed on anterior scalp electrodes[74,75,81,82], with reduced synchronization[75]. This anteriorization of the alpha rhythm was recently also observed with intracranial recordings[83] and may reflect the emergence of this rhythm in isolation of other background activity resulting from more hyperpolarized neurons[84]. In addition, other connections may play a role; for example, frontal-posterior cortico-cortical synchronization was modulated during LOC in animal models[10,51]. Our data showed a clear involvement of frontal areas in arousability but could not separate between these possible pathways.

There is also increased evidence of the therapeutic potential for recovery of consciousness by directly stimulating the thalamus and even indirectly through its pathways, via the PFC. In patients with epilepsy, stimulation of the thalamic pulvinar region improved consciousness scores during seizures[85]. Similarly, responsiveness was briefly restored in monkeys[51,86,87] and in rodent models of focal epilepsy with thalamic stimulation[88,89]. In patients with disorders of consciousness, a clinical study demonstrated that central thalamic stimulation resulted in sustained and reliable functional restoration of consciousness in a patient who had remained in a minimum consciousness state for six years[90]. The authors interpreted the success in arousal as reflecting stimulation “compensating the arousal regulation that is normally controlled by the frontal lobe in the intact brain”[90]. In line

with this, transcranial direct current stimulation targeting the dorsolateral PFC achieved transient improvement[91], which was further sustained with repeated sessions[92]. The major involvement of the PFC in cortico-subcortical networks and its dense connections to the thalamus make it a good target for non-invasive stimulation for disorders of consciousness[93]. This aligns with animal studies that showed that direct stimulation of the PFC prelimbic area but not stimulation of posterior regions restored responsiveness in anesthetized rodents, whereas both PFC and posterior stimulation restored EEG activation[9]. The fact that we observed alteration in functional measures in frontal cortices even with a single pulse further emphasizes these possible mechanisms of action. Future studies based on our protocol in participants with electrodes in the PFC and in the thalamus[94–96] could help further dissociate these mechanisms in humans. Recognizing the brain's distinct response to stimulation during different states not only improves our understanding of the mechanisms of consciousness and arousability but also has direct therapeutic implications. Chronic neuromodulation is increasingly common for movement disorders[17–19,97–100], epilepsy[21,23], and psychiatric disorders[24,101,102], with deep brain stimulation affecting sleep as well[103–105]. Our results showed that even a single brief electrical impulse resulted in different relative connectivity depending on the state of the brain during delivery and where it was delivered, highlighting the need for further research on the effect of stimulation on sleep and other unconscious states.

Each measure has its own strength and limitations, corresponding to different analysis levels; together, they provide a comprehensive understanding of the electrophysiological involvement of the PFC in arousability. Perturbational complexity and CCEP connectivity provide a single value per stimulation channel while response amplitude, outdegree, and variability were computed per recording channel, regardless of where stimulation was delivered. The reduction in complexity during unconscious states was in agreement with transcranial magnetic stimulation (TMS)-EEG studies during sleep, anesthetic-induced LOC, and in disorder of consciousness[58,59,106]. Even at the individual level, the maximum PCI and the network density were larger for conscious vs. unconscious states (Fig 2.f) as in TMS-EEG studies[59], but the absolute values were not sufficient to differentiate among states (Fig. S2). Network connectivity is widely used in neuroscience and CCEP research[57,60]. Here we used well-established measures, casual indegree and outdegree centrality, and density. In addition, we compared the amplitude of the response considering channels responsive in any state and channels responsive in all compared states to reduce bias towards states with more responsive channels. In both cases, we observed an overall decrease in amplitude during unconscious states, which was more pronounced during anesthesia than sleep, particularly in the PFC for detected CCEP responses (Fig 3.e). The overall decrease is different from the reported increase in amplitude with electrocorticographic (ECoG) acquisition[107,108] or following TMS[109], likely due to the focal stimulation with a short low-charge single pulse. Notably, during sleep, the amplitude was similar or larger in 18% of channels and induced slow waves of large amplitude[45] were observed in some channels in individual trials (Fig. S3). Furthermore, similar findings were obtained using either the mean instead of the median, or Keller and colleagues' method for detecting responses[32,110], even though this last method considered CCEP in 76% of the recording channels, as compared to 44% with our method (Fig. S6). Variability is a measure that likely captures different

aspects of neuronal activity than connectivity and amplitude analysis. It does not always correspond with the other measures, does not correlate with the distance between stimulation and recording (Fig. S5.b), and changes prevailed during spontaneous activity outside of stimulation (Fig. S5.c). Variability and the lack of synchronization following stimulation were evident even at the single trial level (Fig. S3). Therefore, variability more likely reflects mechanisms downstream from the stimulation itself such as pre/post-synaptic mechanisms, and dendritic or intrinsic neuronal properties. The increase in variability observed here was present in both sleep and anesthesia but, like other measures, was most robust in PFC during anesthesia. Thus, not only is the communication from/to the PFC heavily disrupted during anesthesia but intrinsic neuronal mechanisms are as well. Statistical differences of all measures hold if we include the anterior cingulate and/or central regions in the frontal group. These results also persisted when separating the PFC into subregions. Future studies including a larger number of participants and perhaps higher density recordings could help us more deeply understand subregional contributions to consciousness and arousability.

Inherent to any intracranial study in participants with epilepsy are heterogeneities due to etiology, medication, brain lesions, or previous surgeries. Depth electrode spatial sampling is always limited and defined by clinical needs. Specific to SPES studies in participants with epilepsy is the possibility of evoking delayed (>100ms) interictal epileptiform activity[29,38,111]. To ensure a comparison of physiological activity, we excluded channels within clinical epileptogenic networks and channels with observed post-stimulation evoked or spontaneous interictal discharges. Our strict criteria ensured the comparison of physiological activity but reduced the number of channels studied. Moreover, to mitigate for heterogeneities, we compared arousable and unarousable unconscious states using relative measures, normalized by awake in each patient and environment. The importance of this normalization was evident in the comparison of awake in the EMU vs. OR. There was no statistical difference in the signal-to-noise ratio, similar to other awake CCEP studies[112], but the dispersion was large (Fig. S5.d). Further, the amplitude of the CCEP responses and variability had wide distributions and there were dissimilarities across recording regions. These could be attributed to environmental noise differences between the EMU and OR, changes in medication levels, timespan from the last seizure[113], changes of excitability with the time of the day[114], changes to the iEEG floor noise level due to equipment re-connection in the OR, or the auditory task used to evaluate LOC in the OR, while no study-related audio was present in the EMU. Having relative measures helped controlled against environmental, temporal, and individual heterogeneities.

It is essential to separate the concept of consciousness, from the concept of being arousable or unarousable. In this work, we have followed a long-standing tradition of characterizing sleep as an unconscious state. Yet the fact that there are reported experiences during sleep would argue that it is not an unconscious state per se[115]. We performed our experiments early in the night during non-REM sleep[45,116], which was confirmed with visual and automatic[117] approaches. Perhaps, most important, which we have tried to emphasize here, is that sleep is at least a state of altered consciousness from which, unlike anesthesia, one can be roused through simple external stimuli. It is worth emphasizing again that what we showed is that loss of consciousness, in both sleep and anesthesia, is accompanied by a broad loss of complexity and connectivity with broad increase variability, whereas loss of

arousability under propofol anesthesia is accompanied by a severe loss of complexity and connectivity and a profound variability increase in the prefrontal cortex. In line with this, non-invasive and animal studies suggest that LOC under anesthesia might not be a singular phenomenon but rather involve several distinct shifts that disrupt both the neural correlates of consciousness and those of arousability. In a scalp EEG study, low-dose propofol, during which participants could be aroused, only affected posterior areas, while high-dose propofol, preventing arousal, resulted in frontal area disruption[118]. Similarly, primate work showed PFC disconnection during deep anesthesia induced by propofol[10]. Our results expand on this differentiation, showing with direct intracranial recording that clinical doses of propofol prevents the PFC from activating, which appears necessary for arousal.

Moreover, although there is discussion of regional differences in trying to understand the mechanisms of consciousness, most theories highlight an integrated, distributed, and interdependent model of consciousness[119]. While we emphasized the lack of PFC responses during propofol-induced anesthesia, suggestive of its role in the unarousable nature of anesthesia, we observed a reduction of information integration and transfer with respect to wake in all regions. We studied the effects of propofol, the most commonly used anesthetic during surgery, but other anesthetic drugs induce different brain dynamics in different brain regions via distinct neural circuit mechanisms[120,121]. A possible future direction to further disentangle and unify the theories of consciousness is to perform a similar protocol as in this study while participants perform different perception tasks, during restful wake, during sleep, and under various drug-induced LOC. Having the entire spectrum with the appropriate normalizing factors could further help understand the neural correlates of consciousness.

In summary, we showed differential cortical network engagement dependent on the state of arousability and consciousness, with the PFC particularly affected by propofol anesthesia. Compared to wake, information integration and transfer were reduced, and response variability increased during any type of loss of consciousness. Still, these differences were more pronounced during anesthesia than sleep with distinct cortical involvement. Indeed, relative inter-trial variability increased, while complexity and response amplitude decreased during anesthesia compared to sleep predominantly in the PFC. This is suggestive of different neural correlations and mechanisms for arousable and unarousable unconscious states, which is a step towards a better understanding of the neural correlates of lack of arousability and loss of consciousness, with significant therapeutic and diagnostic implications.

STAR Methods

Differential Cortical Network Engagement During States of Un/Consciousness

RESOURCE AVAILABILITY

Lead contact—Further information and requests for resources and reagents should be directed to and will be fulfilled by the lead contact, Rina Zelmann (rzelmann@mgh.harvard.edu).

Materials availability—This study did not generate new unique reagents.

Data and Code Availability Statement

- De-identified human/patient standardized datatype data have been deposited at Data Archive BRAIN Initiative (DABI, https://dabi.loni.usc.edu/home). They are publicly available as of the date of publication. Accession numbers are listed in the key resources table.
- All original analysis and visualization code has been deposited at a GitHub repository (https://github.com/Center-For-Neurotechnology/CCEPLOC) and is publicly available as of the date of publication. DOIs are listed in the key resources table.
- Any additional information required to reanalyze the data reported in this paper is available from the lead contact upon request.

EXPERIMENTAL MODEL AND SUBJECT DETAILS

Human Participants—Twenty-three patients with semi-chronic depth electrodes participated in this study. Three of them were excluded: One because of an unrelated clinical situation in the operating room (OR); another one due to widespread pathological activation during anesthesia induction; and another one because only the temporal lobes were implanted. Thus, data from 20 participants were included in the analysis. In 13 participants, stimulation tests were performed while awake and asleep in the epilepsy monitoring unit (EMU), in 14 while awake and under propofol-induced general anesthesia in the OR during the depth-electrode explantation procedure, and in 13 while awake in the EMU and the OR. Seven participants were tested in all states. Participants received their typical antiepileptic medications before the stimulation experiment. A subset of the data obtained during the awake state in the EMU was used in our previous publication[122]. See Table S1 for more details.

Intracerebral Electrodes—Electrodes were implanted exclusively for clinical reasons at the Massachusetts General Hospital (MGH) or Brigham and Women's Hospital (BWH). Depth electrodes (Ad-tech Medical, Racine WI, USA, or PMT, Chanhassen, MN, USA) with diameters of 0.8–1.27 mm and consisting of 4–16 platinum/iridium-contacts 1–2.4 mm long with inter-contact spacing ranging from 4–10 mm (median 5 mm) were stereotactically placed in locations deemed necessary for seizure localization by a multidisciplinary clinical team independent of this research. Following implant, the preoperative T1-weighted MRI was aligned with a postoperative CT or MRI using volumetric image co-registration procedures and FreeSurfer scripts[123,124] (https://surfer.nmr.mgh.harvard.edu/). Electrode coordinates were manually determined from the CT or MRI in the patients' native space. Each contact was assigned an anatomical region from a standardized cortical map, using an electrode labeling algorithm[126,127]. The image processing pipeline is described in detail in[125].

Neural Stimulation and Recordings—Single pulse electrical intracranial stimulation was delivered with a CereStim R96 stimulator (Blackrock Microsystems, Salt Lake City, UT) while simultaneously acquiring intracranial EEG (iEEG) with a Blackrock Neural Signal Processing system at a 2 kHz sampling rate (Blackrock Microsystems, Salt Lake City,

UT, USA). Depth recordings were acquired with reference to an EEG electrode placed on the skin (C2 vertebra or Cz), a chest EEG lead contact, or via an internal ground. Individual charged-balanced biphasic stimulation pulses were 233 μs duration, 90 μs long each phase with 53 μs interstimulus interval[33,122]. The current intensity was 7 mA, the inter-stimulation interval was 2–5 s with +/−0.25 s jitter during wake and sleep in the EMU and 5 +/− 0.25 s during wake and anesthesia in the OR. Current injection and return paths used neighboring contacts in a bipolar configuration. Stimulation was pseudo-randomly delivered to 4–18 stimulation sites, controlled via a custom Cerestim API (https://github.com/Center-For-Neurotechnology/CereLAB) via MATLAB or a custom C++ code. Between 10–30 trials per stimulation site per state were delivered. After the removal of trials with artifacts, the mean +/− standard deviation number of trials was: awake (in the EMU) =17+/−5; sleep= 17+/−6; awake (in the OR) =16+/−5; anesthesia=18+/−6. See Table S1 for the mean number of stimulation trials analyzed per participant and state. A trained electroencephalographer examined continuous recordings for epileptiform activity and asked participants if they experienced any sensations. During the wake sessions, the participants were aware that they were being stimulated but were blind to the stimulation timing and locations.

Ethics statement—All patients voluntarily participated after fully informed consent according to NIH and Army Human Research Protection Office (HRPO) guidelines as monitored by Partners' Institutional Review Board (IRB). Participants were informed that participation in the tests would not alter their clinical treatment and that they could withdraw at any time without jeopardizing their clinical care.

METHOD DETAILS

Channel Selection criteria—For this study, the inclusion criteria were the following: i) contacts inside the parenchyma as assessed from visual inspection of the registered pre- and post-implantation images; ii) channels with iEEG activity as indicated by the expert's report and confirmed by visual inspection of ongoing activity. iii) To focus on physiological responses, channels in the seizure onset zone or in the irritative zone as defined by the clinical team, and channels with stimulation evoked late (>100 ms) transient epileptic activity were excluded. Channels classified primarily as in white matter were included, as they could still record EEG activity. Moreover, stimulation in the white matter produced responses in more distant regions than stimulation exclusively in gray matter[122]. We considered a channel in white matter if 95% of their voxels were classified as white matter. For channels with stimulation, trials within 7.5 s after stimulation were discarded to ensure the amplifiers had settled. For all channels, individual trials with artifacts were discarded if the absolute amplitude exceeded 5 mV or if the z-scored amplitude exceeded 20 in 20% or less of the trials. If it occurred more, the channel was re-evaluated to separate channels with large responses from channels not recording brain activity. After artifact rejection, channels with at least five remaining trials were included. Furthermore, stimulation channels with at least five connected (responsive) channels in any state were included. For example, if delivering stimulation to channel A in p1 resulted in five channels with responses during awake in the EMU, two during sleep, and four during awake in the OR, all those sessions were included. This inclusion criteria ensure comparing stimulation that elicited response under one condition and no other, while removing sessions with no responses whatsoever.

A total of s=115 stimulation channels were included (1–12 per participant) and a total of r=2357 recording channels (29–177 per participant). Table S1 and Supplementary Figure S1 show detailed information on each participant's stimulation sites and recording channels.

For the different measures, the inclusion/exclusion criteria were further refined:

- For complexity and CCEP indegree connectivity, no further exclusion was considered.
- For amplitude and variability, recording channels with responses in ANY state were included. In other words, channels with response during awake but not during sleep (or vice versa) were included. This is important as channels without a detected response are also informative as one reason might be inter-trial variability in the response to stimulation.
- For outdegree, recording channels with responses in one of the compared states were included.
- In addition, we calculated the peak-to-peak amplitude of the CCEP responses considering ONLY channels with responses in both states. We added this restricted channel selection criterion to compare amplitude while reducing any biased in the results towards a state with more responses. Our original hypothesis and the rationale for this addition was that the amplitude would likely be similar in those cases with responses. However, the amplitude was reduced even in channels with responses in both states.

Determining the time of loss of consciousness (LOC) in the OR—The stimulation protocol was delivered in the OR for at least 10 minutes. No anesthetic drugs were administered during the first 5 minutes. During the whole process, from baseline to intubation, patients responded to auditory stimuli (prerecorded words vs. noise) with a button press, and stimuli were presented every 5 s +/− 0.25 jitter[128]. SPES was delivered one second following auditory stimulation.

LOC was evaluated *post-hoc* based on the changes in the spectral content of the ongoing iEEG[81]. This quantitative method ensures the objective determination of the time of LOC. Anesthesia trials were those trials after the LOC time. To exclude a "buffer time", awake trials were defined as trials that occurred 30 seconds before the LOC time.

In the two patients who did not receive propofol and therefore could not be assessed by the spectral analysis method, we only included the awake period in the OR (to add to the comparison with awake in the EMU). In these two cases, we only considered the first 5 minutes of the experiment, in which there was no drug being administered, and they were responsive to the auditory task.

Sleep staging—Sleep sessions occurred at the beginning of the night (day nap for one participant) in the EMU, while the participant was in non-REM (stages N2 or N3) sleep as in[116]. The N2 or N3 sleep stages were visually assessed by a neurologist by the presence of K-complex and spindles on the scalp EEG and intracranial EEG, by the EMG, and by testing

that the patient was not easily awakened. Post-hoc, an automatic algorithm for iEEG sleep staging[129], trained on 8 hours of sleep from a previous night of each patient, confirmed that the patient was asleep, in N2 or N3. In addition, an experienced electroencephalographer visually reviewed the continuous recording and verified the presence of sleep signatures (spindles and k-complexes) and the absence of muscle movement. In a few cases when the algorithm and expert disagreed, the recordings were evaluated for a second time. Of the original 18 patients recorded during the night, 13 were confirmed by both approaches to be asleep and thus included in the study.

QUANTIFICATION AND STATISTICAL ANALYSIS

Intracranial EEG data preprocessing—Data analysis was performed using custom analysis code using MATLAB 2019b and Python. Intracranial EEG (iEEG) was detrended and re-referenced to a bipolar montage created from consecutive contacts within an electrode shaft (referred to as a bipolar channel). A total of 2359 bipolar recording channels were analyzed (Fig. 1 for distribution per patient). The stimulation artifact was then removed using a modified version of the Tukey-windowed median filter method proposed in[130], modified to cover from −1ms to 10ms around the start of the stimulation pulse. This artifact-free signal was filtered with a 100 Hz low pass Butterworth filter, a notch filter at 60 Hz to reduce line noise, and a 0.3 Hz high-pass Butterworth filter. Bipolar filtered iEEG epochs of 1.5 s duration before and after stimulation were analyzed. To ensure comparable amplitude just before stimulation, the iEEG epochs zero mean to [−50 −25] ms for each trial. This signal was used for the variability analysis (see Variability analysis section). This iEEG was then z-score normalized per trial ($perTrial$) with respect to a baseline before each SPES ([−600 to −100ms]).

$$iEEG_{perTrial} = \frac{iEEG - mean(iEEG([-600:-100])}{std(iEEG([-600:-100])}$$

We performed 10–30 trials per site, but some trials were rejected due to environmental noise (e.g., when the patient was intubated) or stimulation artifact railing as detailed above. The median across trials was used for Perturbational complexity and CCEP connectivity measures (see sections Perturbational Complexity and CCEP connectivity). To further control for differences, up to 20 stimulation trials per channel were included in the comparisons. The last up to 20 trials were considered for anesthesia to further ensured we were in the LOC state.

Detection of CCEPs—Cortico-cortical evoked potentials (CCEPs[30]) correspond to the brain's response to single pulse electrical stimulation (SPES[29]) and could be used to create a map of stimulation-responsive networks[34–36]. Exiting CCEP detectors were developed for grids during restful awake and had low specificity[32,110] (Fig. S6). To ensure that connectivity in unconscious states with different background iEEG activity would be captured and that subsequent comparisons would not be biased, we developed the following algorithm to find CCEP responses and generate connectivity networks. We found channels with CCEP response to stimulation during each state in the median of the $perTrial$ normalized lowpass filtered iEEG.

Peak finding.: Find positive and negative peaks during [0 600ms] following SPES using MATLAB *findpeak* function. Peak parameter specifications: i) peak width > 12.5ms; ii) inter-peaks distance > 25ms; iii) peak prominence > 1; iv) the first peak must occur within 300ms of stimulation.

CCEP features.: Compute *peakAmp* measures as i) maximum peak absolute amplitude, ii) peak-to-peak amplitude, similar to[131], and iii) peak-to-peak-to-peak amplitude to account for W-shaped CCEPs. These measures corresponded to CCEP with a large response, a traditional N1-N2 positive-negative response, or a W shape response respectively. The area under the curve was computed in each case as prominence x half-peak width (*peakAUC*).

Baseline peaks.: Create a null distribution of *peakAmp* and *peakAUC* measures for each channel based on randomly selected 100 baseline segments of the same duration as the epoch of interest. The same features as for the epoch following stimulation were computed. The min-max amplitude was considered if no peak was detected for a baseline segment. The 95 quantiles of each null distribution were set as the corresponding threshold for detection ($ThAmpBaseline$ & $ThAUCBaseline$).

Responsive channels.: A recording channel was considered responsive if $RespChPeak = true$ for any CCEP feature:

$$RespChPeak = \left\{ \begin{array}{c} peakAmp > 3 \times ThAmpBaseline\ OR\ peakAUC > 3 \times ThAUCBaseline \\ With \\ eakAmp > thMinAmp\ AND\ peakAUC > thMinAUC \end{array} \right\}$$

Where $peakAmp$ corresponds to peak amplitude, peak-to-peak amplitude, or peak-to-peak-to-peak amplitude; $peakAUC$ corresponds to peak area under the curve (AUC), peak-to-peak AUC, or peak-to-peak-to-peak AUC; thMinAmp was set at Z> 2.576, corresponding to p=0.99 and thMinAUC to 400, corresponding to a minimum 150ms duration for a peak of minimum amplitude. Thresholds for peak-to-peak-to-peak were 2 times larger.

CCEP connectivity measures and features—For each stimulation channel, the percentage of recording channels with a stimulation response was computed. pRespCh = r/R. Where R = total number of channels per participant and r = total number of responsive channels. Thus, $pRespCh$ is the percentage of channels per participant that are responsive. This percentage of responsive channels corresponds to causal indegree connectivity. In addition, the casual outdegree centrality and network density were computed using the Brain Connectivity Toolbox[132]. Outdegree is defined as the number of stimulation sites that produced a response per recording channel, and the density of the network corresponds to the percentage of connections with respect to the number of possible connections. These measures of graph theoretical analysis for neural data have been shown to characterize CCEP networks[32,112].

The amplitude and latency of the CCEPs were computed. More specifically, the max-min amplitude of recording channels responsive under any condition was compared. In addition, to reduce bias towards states with a larger number of responses, we also compared the

peak-to-peak amplitude of detected CCEPs, with responses in all the compared brain states. The latency of the first peak was also compared to ensure that similar events were detected.

Perturbational Complexity – PCIst—The perturbational complexity index (PCI) measures the spatiotemporal complexity in response to a perturbation[42]. PCIst is a version of PCI that could be used in intracranial EEG because it does not require symmetry[52]. Briefly, PCIst computes the spatiotemporal complexity of the EEG by combining dimensionality reduction with principal component analysis (PCA), using single value decomposition, followed by a comparison of transitions following and preceding a perturbation. PCIst was computed per stimulation channel on the mean across trials of the *perTrial* normalized iEEG. The MATLAB implementation of PCIst with default parameters was used, with baseline interval [−700 −100] ms and response interval [0 600] ms, as for CCEP analysis.

Variability Analysis—Inter-stimulation trial variability could be considered a proxy of the intrinsic characteristics of the region from which a channel records. Variability was estimated as the standard deviation (SD) of the filtered (<100Hz) iEEG, [5 to 600] ms following stimulation. SD is a standard measure of inter-trial variability[133]. To include all connected channels to a particular stimulation channel and to reduce noise, we included all recording channels found responsive in any state.

Signal-to-Noise Ratio—The signal-to-noise ratio (SNR) was estimated as the ratio between the variance of the mean across trials of the *perTrial* iEEG in the interval [5 to 600] ms following stimulation divided by the variance in the baseline interval before stimulation [112] (Fig. S5.d).

Relative Measures—One challenge of iEEG recordings is the heterogeneity of implantation sites. Even electrodes aimed at the same anatomical regions would have different trajectories for individual patients, consequently recording from different cortical regions. In addition, the patient's position and environmental noise were different in the EMU and the OR. To compare the loss of consciousness under general anesthesia and sleep, we normalized by the awake state in the corresponding environment.

$$Relative_{State2}^{State1} = \frac{Measure_{State1} - Measure_{State2}}{Measure_{State1} + Measure_{State2}}$$

Where $Measure$ could be PCIst, Connectivity (indegree or outdegree), CCEP Feature, or Variability. $State$ could be anesthesia, sleep, awake in the EMU, or awake in the OR. For instance, the relative connectivity for anesthesia would be

$$RelConnect^{Anesthesia} = \frac{Connectivity_{Anesthesia} - Connectivity_{Awake(OR)}}{Connectivity_{Anesthesia} + Connectivity_{Awake(OR)}}$$

This relative measure is normalized and bounded, with −1 indicating that all the connections that existed during wake were lost during anesthesia, while +1 corresponds to all new connections that appeared during anesthesia. Zero corresponds to the same number of connections in both states. In this way, it was possible to pool measures across patients to

perform comparisons between $RelConnect^{Anesthesia}$ vs. $RelConnect^{Sleep}$, and to compare the effect of stimulation on brain regions.

Statistical Analysis—For the comparison of perturbational complexity and indegree connectivity between states, as comparisons were at the stimulated channel level, and for outdegree connectivity, Wilcoxon signed-rank test was used for paired comparisons and Mann Whitney U-test for unpaired comparisons. For participant wise comparisons between pairs of states, namely maximum PCI and network density, Wilcoxon signed-rank test was used. To assess the linear correlation between measures and with Euclidean Distance, the Pearson correlation was calculated (Fig S5.a–b).

The variability analysis and the features comparisons were performed at the recording channel level with 500–1000 channels in each state. Linear mixed-effects models (LMM) were implemented using data from all participants and states to study how state and other factors affected the dependent variable (amplitude or variability) while controlling for participant-wise variance[134]. Fixed effect models were state, number of trials, location of recording, and location of stimulation channels. Patient identity was the random effect. In other words, the following equation was used, similar to[134]:

$$Feat \approx I + State + \#Trials + RecLoc + StimLoc + \left(\frac{1}{pID}\right) + \left(\frac{\#Trials}{pID}\right) + \left(\frac{RecLoc}{pID}\right) + \left(\frac{StimLoc}{pID}\right)$$

Where $Feat$ corresponded to Amplitude or Variability; $State$ was awake in the EMU, awake in the OR, sleep, or anesthesia; $\#Trials$ was the number of stimulation trials; $RecLoc$ was the anatomical location of the recording channel; StimLoc was the anatomical location of the stimulation channel; and pID was the participant's ID. Note that #Trials, RecLoc, and StimLoc were random predictors of the random effect. To ensure this was a good model, we also compared it to a simpler one without the random predictors (only the fixed effects and 1/pID). There was a significant difference between the models with the more complete model being able to explain more variance. Thus, we report on the above full model. The same conceptual model was implemented to compare relative measures (again for amplitude and variability) for sleep (normalized by awake in the EMU) vs. anesthesia (normalized by awake in the OR). For post-hoc comparisons, permutation tests were used, with the MATLAB implementation from (https://github.com/lrkrol/permutationTest). All other tests were implemented with MATLAB 2019b functions. Significance was set at $p<0.05$.

Regions of interest—The following regions of interest were defined and compared: the *prefrontal* (PFC; Middle frontal, superior frontal, inferior frontal, and orbitofrontal), ii) *posterior* (posterior cingulate, fusiform, parietal, lingual, and occipital cortices), and iii) *temporal* (mesial and lateral temporal) regions. Note that some statistics only included PFC and posterior regions due to the limited number of temporal stimulation channels during anesthesia.

For the anatomical distribution of relative measures (Fig. 3), the following 15 regions were considered: Middle frontal, superior frontal, inferior frontal, orbitofrontal, central, anterior cingulate, isthmus/posterior cingulate, amygdala, hippocampus, insula, temporal, fusiform,

parietal, lingual/occipital, subcortical (nucleus accumbens / caudate / putamen / thalamus). It is important to emphasize that anatomical localization was done in native space, for each participant. Finding anatomical locations in native space ensures higher accuracy.

Plots and Visualizations—Circro plots[135] (Fig. 1, 4 & 6) were created with a modified version of the open-source code (https://github.com/bonilhamusclab/circro). Circro plots were created to illustrate differences in connections and their characteristics at the individual or pooled level. For instance, in Fig. 4 and 6, connections to the different regions from all stimulation originating in PFC (or subregions in Fig. 6) were plotted. In that case, ring colors represented the anatomical region at the lobular or sublobular level (Fig. 4). Circro plots were also created per individual stimulation channels to illustrate differences in CCEP connections and features across states (in Fig. 1.b–e). In those cases, the external ring corresponded to anatomical location, the middle ring to Euclidean distance to stimulation, and the inner ring to the latency of the first peak of the response (Fig. 1). Edges corresponded to CCEP connections, which could be color-coded by amplitude (Fig. 1), individual stimulation channels (Fig. 4&6), or difference of connectivity (Fig. 4).

In addition, relative measures were averaged per region of interest and plotted in stereotaxic space, the Colin27 template[61]. For these visualizations (Fig. 3), the anatomical localization was obtained in native space as detailed above. To visualize individual channels in stereotaxic space (Fig. 1.a, S1, & S4), a non-linear transformation was performed with MMVT software (https://mmvt.mgh.harvard.edu/). This non-linear morphing was only for visualization purposes and not for analysis.

Moreover, CCEP plots were created with in-house software. They illustrated the median value of the *perTrial* normalized EEG, with the color of the line at stimulation time corresponding to the anatomical region of the recording channel (Fig. 1). Epileptic channels were included in these plots for completeness and were indicated with a blue dot; they were not considered in any of the analysis. Channels with detected CCEP response were indicated with a red dot.

Supplementary Material

Refer to Web version on PubMed Central for supplementary material.

Acknowledgments

We would like to thank Dan Soper, Constantin Krempp, and Pariya Salami for their help in data collection. We would like to thank Simone Russo for his advice on PCIst implementation and Tal Benoliel Berman for her help reviewing electrode locations. We would like to especially thank the patients for participating in the study. This work was supported by the Tiny Blue Dot Foundation (RZ, ACP, PLP, DDD, SSC), NIH grant U01NS098968 (RZ, ACP, JDP, BC, SSC), NIH grant K24-NS088568 (SSC), and the CURE Epilepsy Taking Flight award (RZ).

Inclusion and Diversity

One or more of the authors of this paper self-identifies as an underrepresented ethnic minority in their field of research or within their geographical location. One or more of the authors of this paper self-identifies as a gender minority in their field of research.

References

1. Tononi G, Boly M, Massimini M, and Koch C (2016). Integrated information theory: From consciousness to its physical substrate. Nat. Rev. Neurosci. 17, 450–461. 10.1038/nrn.2016.44. [PubMed: 27225071]
2. Koch C, Massimini M, Boly M, and Tononi G (2016). Neural correlates of consciousness: progress and problems. Nat. Rev. Neurosci. 17, 307–321. 10.1038/NRN.2016.22. [PubMed: 27094080]
3. Mashour GA, Roelfsema P, Changeux JP, and Dehaene S (2020). Conscious Processing and the Global Neuronal Workspace Hypothesis. Neuron 105, 776–798. 10.1016/j.neuron.2020.01.026. [PubMed: 32135090]
4. Dehaene S, and Changeux JP (2011). Experimental and Theoretical Approaches to Conscious Processing. Neuron 70, 200–227. 10.1016/J.NEURON.2011.03.018. [PubMed: 21521609]
5. Dehaene S, and Naccache L (2001). Towards a cognitive neuroscience of consciousness: basic evidence and a workspace framework. Cognition 79, 1–37. 10.1016/S0010-0277(00)00123-2. [PubMed: 11164022]
6. Lamme VAF (2010). How neuroscience will change our view on consciousness. Cogn. Neurosci. 1, 204–220. 10.1080/17588921003731586. [PubMed: 24168336]
7. Malach R (2021). Local neuronal relational structures underlying the contents of human conscious experience. Neurosci. Conscious. 2021. 10.1093/NC/NIAB028.
8. Schiff ND (2010). Recovery of consciousness after brain injury: a mesocircuit hypothesis. Trends Neurosci. 33, 1–9. 10.1016/J.TINS.2009.11.002. [PubMed: 19954851]
9. Pal D, Dean JG, Liu T, Li D, Watson CJ, Hudetz AG, and Mashour GA (2018). Differential Role of Prefrontal and Parietal Cortices in Controlling Level of Consciousness. Curr. Biol. 28, 2145–2152.e5. 10.1016/j.cub.2018.05.025. [PubMed: 29937348]
10. Bastos AM, Donoghue JA, Brincat SL, Mahnke M, Yanar J, Correa J, Waite AS, Lundqvist M, Roy J, Brown EN, et al. (2021). Neural effects of propofol-induced unconsciousness and its reversal using thalamic stimulation. Elife 10. 10.7554/ELIFE.60824.
11. Pitkänen A, Ekolle Ndode-Ekane X, Lapinlampi N, and Puhakka N (2019). Epilepsy biomarkers – Toward etiology and pathology specificity. Neurobiol. Dis. 123, 42–58. 10.1016/j.nbd.2018.05.007. [PubMed: 29782966]
12. Boly M, Massimini M, Tsuchiya N, Postle BR, Koch C, and Tononi G (2017). Are the neural correlates of consciousness in the front or in the back of the cerebral cortex? Clinical and neuroimaging evidence. J. Neurosci. 37, 9603–9613. 10.1523/JNEUROSCI.3218-16.2017. [PubMed: 28978697]
13. Odegaard B, Knight RT, and Lau H (2017). Should a few null findings falsify prefrontal theories of conscious perception? J. Neurosci. 37, 9593–9602. 10.1523/JNEUROSCI.3217-16.2017. [PubMed: 28978696]
14. Brown EN, Lydic R, Schiff ND, Schwartz RS, Brown EN, Lydic R, and Schiff ND (2010). General anesthesia, sleep, and coma Schwartz RS, ed. (Massachussetts Medical Society) 10.1056/NEJMra0808281.
15. Bonhomme V, Boveroux P, Vanhaudenhuyse A, Hans P, Brichant JF, Jaquet O, Boly M, and Laureys S (2011). Linking sleep and general anesthesia mechanisms: This is no walkover. Acta Anaesthesiol. Belg. 62, 161–171. [PubMed: 22145259]
16. Mashour GA, and Pal D (2012). Interfaces of Sleep and Anesthesia. Anesthesiol. Clin. 30, 385–398. 10.1016/j.anclin.2012.05.003. [PubMed: 22901616]
17. Lozano AM, Lipsman N, Bergman H, Brown P, Chabardes S, Chang JW, Matthews K, McIntyre CC, Schlaepfer TE, Schulder M, et al. (2019). Deep brain stimulation: current challenges and future directions. 15, 148–160.
18. Bronstein JM, Tagliati M, Alterman RL, Lozano AM, Volkmann J, Stefani A, Horak FB, Okun MS, Foote KD, Krack P, et al. (2011). Deep Brain Stimulation for Parkinson Disease: An Expert Consensus and Review of Key Issues. Arch. Neurol. 68, 165–165. 10.1001/ARCHNEUROL.2010.260. [PubMed: 20937936]
19. Herrington TM, Cheng JJ, and Eskandar EN (2016). Mechanisms of deep brain stimulation. J. Neurophysiol. 115, 19–38. 10.1152/JN.00281.2015. [PubMed: 26510756]

20. Kokkinos V, Sisterson ND, Wozny TA, and Richardson RM (2019). Association of Closed-Loop Brain Stimulation Neurophysiological Features With Seizure Control Among Patients With Focal Epilepsy. JAMA Neurol. 76, 800. 10.1001/jamaneurol.2019.0658. [PubMed: 30985902]
21. Jarosiewicz B, and Morrell M (2021). The RNS System: brain-responsive neurostimulation for the treatment of epilepsy. Expert Rev. Med. Devices 18, 129–138. 10.1080/17434440.2019.1683445.
22. Ryvlin P, Rheims S, Hirsch LJ, Sokolov A, and Jehi L (2021). Neuromodulation in epilepsy: state-of-the-art approved therapies. Lancet. Neurol. 20, 1038–1047. 10.1016/S1474-4422(21)00300-8. [PubMed: 34710360]
23. Salanova V, Sperling MR, Gross RE, Irwin CP, Vollhaber JA, Giftakis JE, and Fisher RS (2021). The SANTÉ study at 10 years of follow-up: Effectiveness, safety, and sudden unexpected death in epilepsy. Epilepsia 62, 1306–1317. 10.1111/EPI.16895. [PubMed: 33830503]
24. Holtzheimer PE, and Mayberg HS (2011). Deep brain stimulation for psychiatric disorders. Annu. Rev. Neurosci. 34, 289–307. 10.1146/ANNUREV-NEURO-061010-113638. [PubMed: 21692660]
25. Mayberg HS, Lozano AM, Voon V, McNeely HE, Seminowicz D, Hamani C, Schwalb JM, and Kennedy SH (2005). Deep brain stimulation for treatment-resistant depression. Neuron 45, 651–660. 10.1016/J.NEURON.2005.02.014/ATTACHMENT/27415A16-5464-48A0-824B-A0DA236C5051/MMC1.PDF. [PubMed: 15748841]
26. Widge AS, Malone DA, and Dougherty DD (2018). Closing the Loop on Deep Brain Stimulation for Treatment-Resistant Depression. Front. Neurosci. 12, 175. 10.3389/fnins.2018.00175. [PubMed: 29618967]
27. Basu I, Yousefi A, Crocker B, Zelmann R, Paulk AC, Peled N, Ellard KK, Weisholtz DS, Cosgrove GR, Deckersbach T, et al. (2021). Closed-loop enhancement and neural decoding of cognitive control in humans. Nat. Biomed. Eng. 10.1038/s41551-021-00804-y.
28. PENFIELD W, and BOLDREY E (1937). SOMATIC MOTOR AND SENSORY REPRESENTATION IN THE CEREBRAL CORTEX OF MAN AS STUDIED BY ELECTRICAL STIMULATION1. Brain 60, 389–443. 10.1093/brain/60.4.389.
29. Valentín A, Anderson M, Alarcón G, Seoane JJG, Selway R, Binnie CD, and Polkey CE (2002). Responses to single pulse electrical stimulation identify epileptogenesis in the human brain in vivo. Brain 125, 1709–1718. [PubMed: 12135963]
30. Matsumoto R, Nair DR, LaPresto E, Najm I, Bingaman W, Shibasaki H, and Lüders HO (2004). Functional connectivity in the human language system: a cortico-cortical evoked potential study. Brain 127, 2316–2330. 10.1093/brain/awh246. [PubMed: 15269116]
31. Matsumoto R, Nair DR, LaPresto E, Bingaman W, Shibasaki H, Luders HO, and Lüders HO (2006). Functional connectivity in human cortical motor system: a cortico-cortical evoked potential study. Brain 130, 181–197. 10.1093/brain/awl257. [PubMed: 17046857]
32. Keller CJ, Honey CJ, Entz L, Bickel S, Groppe DM, Toth E, Ulbert I, Lado FA, and Mehta AD (2014). Corticocortical evoked potentials reveal projectors and integrators in human brain networks. J. Neurosci. 34, 9152–9163. 10.1523/JNEUROSCI.4289-13.2014. [PubMed: 24990935]
33. Crocker B, Ostrowski L, Williams ZM, Dougherty DD, Eskandar EN, Widge AS, Chu CJ, Cash SS, and Paulk AC (2021). Local and distant responses to single pulse electrical stimulation reflect different forms of connectivity. Neuroimage 237. 10.1016/J.NEUROIMAGE.2021.118094.
34. David O, Job AS, De Palma L, Hoffmann D, Minotti L, and Kahane P (2013). Probabilistic functional tractography of the human cortex. Neuroimage 80, 307–317. [PubMed: 23707583]
35. Trebaul L, Deman P, Tuyisenge V, Jedynak M, Hugues E, Rudrauf D, Bhattacharjee M, Tadel F, Chanteloup-Foret B, Saubat C, et al. (2018). Probabilistic functional tractography of the human cortex revisited. Neuroimage. 10.1016/j.neuroimage.2018.07.039.
36. Matsumoto R, Kunieda T, and Nair D (2017). Single pulse electrical stimulation to probe functional and pathological connectivity in epilepsy. Seizure 44, 27–36. 10.1016/j.seizure.2016.11.003. [PubMed: 27939100]
37. Kokkinos V, Alarcón G, Selway RP, and Valentín A (2013). Role of single pulse electrical stimulation (SPES) to guide electrode implantation under general anaesthesia in presurgical assessment of epilepsy. Seizure 22, 198–204. [PubMed: 23298606]
38. Valentín A, Alarcón G, García-Seoane JJ, Lacruz ME, Nayak SD, Honavar M, Selway RP, Binnie CD, and Polkey CE (2005). Single-pulse electrical stimulation identifies epileptogenic

frontal cortex in the human brain. Neurology 65, 426–435. 10.1212/01.wnl.0000171340.73078.c1. [PubMed: 16087908]

39. Flanagan D, Valentín A, García Seoane JJ, Alarcón G, and Boyd SG (2009). Single-pulse electrical stimulation helps to identify epileptogenic cortex in children. Epilepsia 50, 1793–1803. 10.1111/j.1528-1167.2009.02056.x. [PubMed: 19453705]
40. Yamao Y, Matsumoto R, Kikuchi T, Yoshida K, Kunieda T, and Miyamoto S (2021). Intraoperative Brain Mapping by Cortico-Cortical Evoked Potential. Front. Hum. Neurosci. 15, 635453. 10.3389/fnhum.2021.635453. [PubMed: 33679353]
41. Bourdillon P, Hermann B, Guénot M, Bastuji H, Isnard J, King JR, Sitt J, and Naccache L (2020). Brain-scale cortico-cortical functional connectivity in the delta-theta band is a robust signature of conscious states: an intracranial and scalp EEG study. Sci. Rep. 10. 10.1038/s41598-020-70447-7.
42. Casali AG, Gosseries O, Rosanova M, Boly M, Sarasso S, Casali KR, Casarotto S, Bruno MA, Laureys S, Tononi G, et al. (2013). A theoretically based index of consciousness independent of sensory processing and behavior.
43. Sarasso S, Rosanova M, Casali AG, Casarotto S, Fecchio M, Boly M, Gosseries O, Tononi G, Laureys S, and Massimini M (2014). Quantifying cortical EEG responses to TMS in (un)consciousness. Clin. EEG Neurosci. 45, 40–49. 10.1177/1550059413513723. [PubMed: 24403317]
44. Massimini M, Boly M, Casali A, Rosanova M, and Tononi G (2009). A perturbational approach for evaluating the brain's capacity for consciousness. Prog. Brain Res. 177, 201–214. 10.1016/S0079-6123(09)17714-2. [PubMed: 19818903]
45. Pigorini A, Sarasso S, Proserpio P, Szymanski C, Arnulfo G, Casarotto S, Fecchio M, Rosanova M, Mariotti M, Lo Russo G, et al. (2015). Bistability breaks-off deterministic responses to intracortical stimulation during non-REM sleep. Neuroimage 112, 105–113. 10.1016/J.NEUROIMAGE.2015.02.056. [PubMed: 25747918]
46. Sarasso S, Boly M, Napolitani M, Gosseries O, Charland-Verville V, Casarotto S, Rosanova M, Casali AG, Brichant JF, Boveroux P, et al. (2015). Consciousness and complexity during unresponsiveness induced by propofol, xenon, and ketamine. Curr. Biol. 25, 3099–3105. 10.1016/j.cub.2015.10.014. [PubMed: 26752078]
47. Rosanova M, Gosseries O, Casarotto S, Boly M, Casali AG, Bruno M-A, Mariotti M, Boveroux P, Tononi G, Laureys S, et al. (2012). Recovery of cortical effective connectivity and recovery of consciousness in vegetative patients. Brain 135, 1308–1320. 10.1093/brain/awr340. [PubMed: 22226806]
48. Krom AJ, Marmelshtein A, Gelbard-Sagiv H, Tankus A, Hayat H, Hayat D, Matot I, Strauss I, Fahoum F, Soehle M, et al. (2020). Anesthesia-induced loss of consciousness disrupts auditory responses beyond primary cortex. Proc. Natl. Acad. Sci. U. S. A. 117. 10.1073/PNAS.1917251117.
49. Tononi G (2012). Integrated information theory of consciousness: an updated account. Arch. Ital. Biol. 150, 293–329. 10.4449/AIB.V149I5.1388. [PubMed: 23802335]
50. Pal D, Silverstein BH, Lee H, and Mashour GA (2016). Neural Correlates of Wakefulness, Sleep, and General Anesthesia: An Experimental Study in Rat. Anesthesiology 125, 929–942. 10.1097/ALN.0000000000001342. [PubMed: 27617688]
51. Redinbaugh MJ, Phillips JM, Kambi NA, Mohanta S, Andryk S, Dooley GL, Afrasiabi M, Raz A, and Saalmann YB (2020). Thalamus Modulates Consciousness via Layer-Specific Control of Cortex. Neuron 106, 66–75.e12. 10.1016/j.neuron.2020.01.005. [PubMed: 32053769]
52. Comolatti R, Pigorini A, Casarotto S, Fecchio M, Faria G, Sarasso S, Rosanova M, Gosseries O, Boly M, Bodart O, et al. (2019). A fast and general method to empirically estimate the complexity of brain responses to transcranial and intracranial stimulations. Brain Stimul. 10.1016/j.brs.2019.05.013.
53. Sarasso S, Casali AG, Casarotto S, Rosanova M, Sinigaglia C, and Massimini M (2021). Consciousness and complexity: a consilience of evidence. Neurosci. Conscious. 2021, 1–24. 10.1093/NC/NIAB023.

54. Sergent C, Corazzol M, Labouret G, Stockart F, Wexler M, King JR, Meyniel F, and Pressnitzer D (2021). Bifurcation in brain dynamics reveals a signature of conscious processing independent of report. Nat. Commun. 12. 10.1038/S41467-021-21393-Z.
55. Arieli A, Sterkin A, Grinvald A, and Aertsen A (1996). Dynamics of ongoing activity: explanation of the large variability in evoked cortical responses. Science 273, 1868–1871. 10.1126/SCIENCE.273.5283.1868. [PubMed: 8791593]
56. Fox MD, Snyder AZ, Vincent JL, and Raichle ME (2007). Intrinsic Fluctuations within Cortical Systems Account for Intertrial Variability in Human Behavior. Neuron 56, 171–184. 10.1016/J.NEURON.2007.08.023. [PubMed: 17920023]
57. Huang Y, and Keller C How can I investigate causal brain networks with iEEG?
58. Casali AG, Gosseries O, Rosanova M, Boly M, Sarasso S, Casali KR, Casarotto S, Bruno MA, Laureys S, Tononi G, et al. (2013). A theoretically based index of consciousness independent of sensory processing and behavior. Sci. Transl. Med. 5. 10.1126/SCITRANSLMED.3006294.
59. Casarotto S, Comanducci A, Rosanova M, Sarasso S, Fecchio M, Napolitani M, Pigorini A, Casali G, A., Trimarchi PD., Boly M., et al. (2016). Stratification of unresponsive patients by an independently validated index of brain complexity. Ann. Neurol. 80, 718–729. 10.1002/ANA.24779. [PubMed: 27717082]
60. Hays MA, Coogan C, Crone NE, and Kang JY (2021). Graph theoretical analysis of evoked potentials shows network influence of epileptogenic mesial temporal region. Hum. Brain Mapp. 42, 4173–4186. 10.1002/HBM.25418. [PubMed: 34165233]
61. Holmes CJ, Hoge R, Collins L, Woods R, Toga AW, and Evans AC (1998). Enhancement of MR images using registration for signal averaging. J. Comput. Assist. Tomogr. 22, 324–333. 10.1097/00004728-199803000-00032. [PubMed: 9530404]
62. Aubert-Broche B, Evans AC, and Collins L (2006). A new improved version of the realistic digital brain phantom. Neuroimage 32, 138–145. 10.1016/J.NEUROIMAGE.2006.03.052. [PubMed: 16750398]
63. Brown EN, Purdon PL, and Van Dort CJ (2011). General anesthesia and altered states of arousal: a systems neuroscience analysis. Annu. Rev. Neurosci. 34, 601–628. 10.1146/ANNUREV-NEURO-060909-153200. [PubMed: 21513454]
64. Goodchild CS, and Serrao JM (1989). Cardiovascular effects of propofol in the anaesthetized dog. Br. J. Anaesth. 63, 87–92. 10.1093/BJA/63.1.87. [PubMed: 2788450]
65. Song C, Boly M, Tagliazucchi E, Laufs H, and Tononi G (2022). fMRI spectral signatures of sleep. Proc. Natl. Acad. Sci. U. S. A. 119. 10.1073/PNAS.2016732119.
66. von Ellenrieder N, Gotman J, Zelmann R, Rogers C, Nguyen DKDK, Kahane P, Dubeau F, and Frauscher B (2020). How the Human Brain Sleeps: Direct Cortical Recordings of Normal Brain Activity. Ann. Neurol. 87, 289–301. 10.1002/ana.25651. [PubMed: 31777112]
67. Frauscher B, and Gotman J (2019). Sleep, oscillations, interictal discharges, and seizures in human focal epilepsy. Neurobiol. Dis. 127, 545–553. 10.1016/j.nbd.2019.04.007. [PubMed: 30981828]
68. Siclari F, and Tononi G (2017). Local aspects of sleep and wakefulness. Curr. Opin. Neurobiol. 44, 222–227. 10.1016/J.CONB.2017.05.008. [PubMed: 28575720]
69. Steriade M, McCormick DA, and Sejnowski TJ (1993). Thalamocortical oscillations in the sleeping and aroused brain. 262, 679–685.
70. Steriade M, and Timofeev I (2003). Neuronal plasticity in thalamocortical networks during sleep and waking oscillations. Neuron 37, 563–576. 10.1016/S0896-6273(03)00065-5. [PubMed: 12597855]
71. Piantoni G, Halgren E, and Cash SS (2016). The Contribution of Thalamocortical Core and Matrix Pathways to Sleep Spindles. Neural Plast. 2016. 10.1155/2016/3024342.
72. Giacino JT, Fins JJ, Laureys S, and Schiff ND (2014). Disorders of consciousness after acquired brain injury: The state of the science. Nat. Rev. Neurol. 10, 99–114. 10.1038/nrneurol.2013.279. [PubMed: 24468878]
73. Schiff ND (2008). Central thalamic contributions to arousal regulation and neurological disorders of consciousness. Ann. N. Y. Acad. Sci. 1129, 105–118. 10.1196/annals.1417.029. [PubMed: 18591473]

74. Lewis LD, Weiner VS, Mukamel EA, Donoghue JA, Eskandar EN, Madsen JR, Anderson WS, Hochberg LR, Cash SS, Brown EN, et al. (2012). Rapid fragmentation of neuronal networks at the onset of propofol-induced unconsciousness. Proc. Natl. Acad. Sci. U. S. A. 109. 10.1073/pnas.1210907109.

75. Flores FJ, Hartnack KE, Fath AB, Kim SE, Wilson MA, Brown EN, and Purdon PL (2017). Thalamocortical synchronization during induction and emergence from propofol-induced unconsciousness. Proc. Natl. Acad. Sci. U. S. A. 114, E6660–E6668. 10.1073/PNAS.1700148114. [PubMed: 28743752]

76. Schwartz RS, Brown EN, Lydic R, and Schiff ND (2010). Mechanisms of Disease General Anesthesia, Sleep, and Coma.

77. Ma L, Liu W, and Hudson AE (2019). Propofol Anesthesia Increases Long-range Frontoparietal Corticocortical Interaction in the Oculomotor Circuit in Macaque Monkeys. Anesthesiology 130, 560–571. 10.1097/ALN.0000000000002637. [PubMed: 30807382]

78. Liu X, Lauer KK, Ward BD, Li SJ, and Hudetz AG (2013). Differential effects of deep sedation with propofol on the specific and nonspecific thalamocortical systems: a functional magnetic resonance imaging study. Anesthesiology 118, 59–69. 10.1097/ALN.0B013E318277A801. [PubMed: 23221862]

79. Mashour GA, and Alkire MT (2013). Consciousness, Anesthesia, and the thalamocortical system. Anesthesiology 118, 13–15. 10.1097/ALN.0b013e318277a9c6. [PubMed: 23208518]

80. Purdon PL, Sampson A, Pavone KJ, and Brown EN (2015). Clinical Electroencephalography for Anesthesiologists: Part I: Background and Basic Signatures. Anesthesiology 123, 937–960. 10.1097/ALN.0000000000000841. [PubMed: 26275092]

81. Purdon PL, Pierce ET, Mukamel EA, Prerau MJ, Walsh JL, Wong KFK, Salazar-Gomez AF, Harrell PG, Sampson AL, Cimenser A, et al. (2013). Electroencephalogram signatures of loss and recovery of consciousness from propofol. Proc. Natl. Acad. Sci. U. S. A. 110. 10.1073/PNAS.1221180110.

82. Ching SN, and Brown EN (2014). Modeling the dynamical effects of anesthesia on brain circuits. Curr. Opin. Neurobiol. 25, 116–122. 10.1016/j.conb.2013.12.011. [PubMed: 24457211]

83. Weiner VS, Zhou DW, Kahali P, Stephen EP, Peterfreund RA, Aglio LS, Szabo MD, Eskandar EN, Salazar-Gomez AF, Sampson AL, et al. (2023). Propofol disrupts alpha dynamics in functionally distinct thalamocortical networks during loss of consciousness. Proc. Natl. Acad. Sci. U. S. A. 120. 10.1073/PNAS.2207831120.

84. Vijayan S, Ching SN, Purdon PL, Brown EN, and Kopell NJ (2013). Thalamocortical mechanisms for the anteriorization of α rhythms during propofol-induced unconsciousness. J. Neurosci. 33, 11070–11075. 10.1523/JNEUROSCI.5670-12.2013. [PubMed: 23825412]

85. Filipescu C, Lagarde S, Lambert I, Pizzo F, Trébuchon A, McGonigal A, Scavarda D, Carron R, and Bartolomei F (2019). The effect of medial pulvinar stimulation on temporal lobe seizures. Epilepsia 60, e25–e30. 10.1111/EPI.14677. [PubMed: 30767195]

86. Bastos AM, and Schoffelen JM (2016). A tutorial review of functional connectivity analysis methods and their interpretational pitfalls. Front. Syst. Neurosci. 9. 10.3389/fnsys.2015.00175.

87. Tasserie J, Uhrig L, Sitt JD, Manasova D, Dupont M, Dehaene S, and Jarraya B (2022). Deep brain stimulation of the thalamus restores signatures of consciousness in a nonhuman primate model. 8, 5547.

88. Xu J, Galardi MM, Pok B, Patel KK, Zhao CW, Andrews JP, Singla S, McCafferty CP, Feng L, Musonza ET, et al. (2020). Thalamic stimulation improves postictal cortical arousal and behavior. J. Neurosci. 40, 7343–7354. 10.1523/JNEUROSCI.1370-20.2020. [PubMed: 32826310]

89. Gummadavelli A, Motelow JE, Smith N, Zhan Q, Schiff ND, and Blumenfeld H (2015). Thalamic stimulation to improve level of consciousness after seizures: evaluation of electrophysiology and behavior. Epilepsia 56, 114–124. 10.1111/EPI.12872. [PubMed: 25442843]

90. Schiff ND, Giacino JT, Kalmar K, Victor JD, Baker K, Gerber M, Fritz B, Eisenberg B, O'Connor J, Kobylarz EJ, et al. (2007). Behavioural improvements with thalamic stimulation after severe traumatic brain injury. Nature 448, 600–603. 10.1038/NATURE06041. [PubMed: 17671503]

91. Thibaut A, Bruno MA, Ledoux D, Demertzi A, and Laureys S (2014). tDCS in patients with disorders of consciousness: sham-controlled randomized double-blind study. Neurology 82, 1112–1118. 10.1212/WNL.0000000000000260. [PubMed: 24574549]

92. Thibaut A, Wannez S, Donneau AF, Chatelle C, Gosseries O, Bruno MA, and Laureys S (2017). Controlled clinical trial of repeated prefrontal tDCS in patients with chronic minimally conscious state. Brain Inj. 31, 466–474. 10.1080/02699052.2016.1274776. [PubMed: 28281845]

93. Bourdillon P, Hermann B, Sitt JD, and Naccache L (2019). Electromagnetic Brain Stimulation in Patients With Disorders of Consciousness. Front. Neurosci. 13. 10.3389/FNINS.2019.00223.

94. Arthuis M, Valton L, Ré J, Chauvel P, Wendling F, Naccache L, Bernard C, Bartolomei F, Rgis J, Chauvel P, et al. (2009). Impaired consciousness during temporal lobe seizures is related to increased long-distance cortical-subcortical synchronization. 132, 2091–2101.

95. Chaitanya G, Sinha S, Narayanan M, and Satishchandra P (2015). Scalp high frequency oscillations (HFOs) in absence epilepsy: An independent component analysis (ICA) based approach. Epilepsy Res. 115, 133–140. 10.1016/j.eplepsyres.2015.06.008. [PubMed: 26220390]

96. Blumenfeld H (2021). Arousal and Consciousness in Focal Seizures. Epilepsy Curr. 21, 353–359. 10.1177/15357597211029507. [PubMed: 34924835]

97. Lozano AM, Hutchison WD, and Kalia SK (2017). What Have We Learned About Movement Disorders from Functional Neurosurgery? Annu. Rev. Neurosci. 40, 453–477. 10.1146/ANNUREV-NEURO-070815-013906. [PubMed: 28772097]

98. Eisinger RS, Cernera S, Gittis A, Gunduz A, and Okun MS (2019). A review of basal ganglia circuits and physiology: Application to deep brain stimulation. Parkinsonism Relat. Disord. 59, 9–20. 10.1016/J.PARKRELDIS.2019.01.009. [PubMed: 30658883]

99. Krack P, Volkmann J, Tinkhauser G, and Deuschl G (2019). Deep Brain Stimulation in Movement Disorders: From Experimental Surgery to Evidence-Based Therapy. Mov. Disord. 34, 1795–1810. 10.1002/MDS.27860. [PubMed: 31580535]

100. Benabid AL, Chabardes S, Torres N, Piallat B, Krack P, Fraix V, and Pollak P (2009). Functional neurosurgery for movement disorders: a historical perspective. Prog. Brain Res. 175, 379–391. 10.1016/S0079-6123(09)17525-8. [PubMed: 19660668]

101. Widge AS, Ellard KK, Paulk AC, Basu I, Yousefi A, Zorowitz S, Gilmour A, Afzal A, Deckersbach T, Cash SS, et al. (2017). Treating refractory mental illness with closed-loop brain stimulation: Progress towards a patient-specific transdiagnostic approach. Exp. Neurol. 287, 461–472. 10.1016/J.EXPNEUROL.2016.07.021. [PubMed: 27485972]

102. Lee MB, Kramer DR, Peng T, Barbaro MF, Liu CY, Kellis S, and Lee B (2019). Clinical neuroprosthetics: Today and tomorrow. J. Clin. Neurosci. 10.1016/j.jocn.2019.07.056.

103. Dafsari HS, Ray-Chaudhuri K, Ashkan K, Sachse L, Mahlstedt P, Silverdale M, Rizos A, Strack M, Jost ST, Reker P, et al. (2020). Beneficial effect of 24-month bilateral subthalamic stimulation on quality of sleep in Parkinson's disease. J. Neurol. 267, 1830–1841. 10.1007/S00415-020-09743-1. [PubMed: 32152689]

104. Jost ST, Ray Chaudhuri K, Ashkan K, Loehrer PA, Silverdale M, Rizos A, Evans J, Petry-Schmelzer JN, Barbe MT, Sauerbier A, et al. (2021). Subthalamic stimulation improves quality of sleep in Parkinson disease: A 36-month controlled study. J. Parkinsons. Dis. 11, 323–335. 10.3233/JPD-202278. [PubMed: 33074192]

105. Zuzuárregui JRP, and Ostrem JL (2020). The Impact of Deep Brain Stimulation on Sleep in Parkinson's Disease: An update. J. Parkinsons. Dis. 10, 393–404. 10.3233/JPD-191862. [PubMed: 32250316]

106. Schartner MM, Pigorini A, Gibbs SA, Arnulfo G, Sarasso S, Barnett L, Nobili L, Massimini M, Seth AK, and Barrett AB (2017). Global and local complexity of intracranial EEG decreases during NREM sleep. Neurosci. Conscious. 2017, 1–12. 10.1093/NC/NIW022.

107. Usami K, Matsumoto R, Kobayashi K, Hitomi T, Shimotake A, Kikuchi T, Matsuhashi M, Kunieda T, Mikuni N, Miyamoto S, et al. (2015). Sleep modulates cortical connectivity and excitability in humans: Direct evidence from neural activity induced by single-pulse electrical stimulation. Hum. Brain Mapp. 36, 4714–4729. 10.1002/HBM.22948. [PubMed: 26309062]

108. Suzuki Y, Enatsu R, Kanno A, Yokoyama R, Suzuki H, Tachibana S, Akiyama Y, Mikami T, Ochi S, Yamakage M, et al. (2019). The Influence of Anesthesia on Corticocortical Evoked

Potential Monitoring Network Between Frontal and Temporoparietal Cortices. World Neurosurg. 123, e685–e692. 10.1016/J.WNEU.2018.11.253. [PubMed: 30576824]

109. Ferrarelli F, Massimini M, Sarasso S, Casali A, Riedner BA, Angelini G, Tononi G, and Pearce RA (2010). Breakdown in cortical effective connectivity during midazolam-induced loss of consciousness. Proc. Natl. Acad. Sci. U. S. A. 107, 2681–2686. 10.1073/PNAS.0913008107. [PubMed: 20133802]
110. Keller CJ, Bickel S, Entz L, Ulbert I, Milham MP, Kelly C, and Mehta AD (2011). Intrinsic functional architecture predicts electrically evoked responses in the human brain. Proc. Natl. Acad. Sci. U. S. A. 108, 10308–10313. 10.1073/PNAS.1019750108. [PubMed: 21636787]
111. Nayak D, Valentín A, Selway RP, and Alarcón G (2014). Can single pulse electrical stimulation provoke responses similar to spontaneous interictal epileptiform discharges? Clin. Neurophysiol. 125, 1306–1311. 10.1016/j.clinph.2013.11.019. [PubMed: 24424009]
112. Hays MA, Smith RJ, Haridas B, Coogan C, Crone NE, and Kang JY (2021). Effects of stimulation intensity on intracranial cortico-cortical evoked potentials: A titration study. Clin. Neurophysiol. 132, 2766–2777. [PubMed: 34583119]
113. David O, Woźniak A, Minotti L, and Kahane P (2008). Preictal short-term plasticity induced by intracerebral 1 Hz stimulation. Neuroimage 39, 1633–1646. 10.1016/J.NEUROIMAGE.2007.11.005. [PubMed: 18155929]
114. Huber R, Mäki H, Rosanova M, Casarotto S, Canali P, Casali AG, Tononi G, and Massimini M (2013). Human cortical excitability increases with time awake. Cereb. Cortex 23, 332–338. 10.1093/CERCOR/BHS014. [PubMed: 22314045]
115. Sevenius Nilsen A, Juel BE, Thürer B, Aamodt A, and Storm JF (2022). Are we really unconscious in “unconscious” states? Common assumptions revisited. Front. Hum. Neurosci. 16, 678. 10.3389/FNHUM.2022.987051/BIBTEX.
116. Massimini M, Ferrarelli F, Huber R, Esser SK, Singh H, and Tononi G (2005). Breakdown of cortical effective connectivity during sleep. Science 309, 2228–2232. 10.1126/SCIENCE.1117256. [PubMed: 16195466]
117. Von Ellenrieder N, Peter-Derex L, Gotman J, and Frauscher B (2022). SleepSEEG: automatic sleep scoring using intracranial EEG recordings only. J. Neural Eng. 19. 10.1088/1741-2552/AC6829.
118. Stephen EP, Hotan GC, Pierce ET, Harrell G, Walsh JL, Brown EN, Patrick, &, and Purdon L (2020). Broadband slow-wave modulation in posterior and anterior cortex tracks distinct states of propofol-induced unconsciousness. 10.1038/s41598-020-68756-y.
119. Northoff G, and Lamme V (2020). Neural signs and mechanisms of consciousness: Is there a potential convergence of theories of consciousness in sight? Neurosci. Biobehav. Rev. 118, 568–587. 10.1016/J.NEUBIOREV.2020.07.019. [PubMed: 32783969]
120. Purdon PL, Sampson A, Pavone KJ, and Brown EN (2015). Clinical Electroencephalography for Anesthesiologists: Part I: Background and Basic Signatures. Anesthesiology 123, 937–960. 10.1097/ALN.0000000000000841. [PubMed: 26275092]
121. Vesuna S, Kauvar IV, Richman E, Gore F, Oskotsky T, Sava-Segal C, Luo L, Malenka RC, Henderson JM, Nuyujukian P, et al. (2020). Deep posteromedial cortical rhythm in dissociation. Nature 586, 87–94. 10.1038/S41586-020-2731-9. [PubMed: 32939091]
122. Paulk AC, Zelmann R, Crocker B, Widge AS, Dougherty DD, Eskandar EN, Weisholtz DS, Richardson RM, Cosgrove GR, Williams ZM, et al. (2022). Local and distant cortical responses to single pulse intracranial stimulation in the human brain are differentially modulated by specific stimulation parameters. Brain Stimul. 15, 491–508. 10.1016/J.BRS.2022.02.017. [PubMed: 35247646]
123. Dale AM, Fischl B, and Sereno MI (1999). Cortical surface-based analysis. I. Segmentation and surface reconstruction. Neuroimage 9, 179–194. 10.1006/NIMG.1998.0395. [PubMed: 9931268]
124. Fischl B, Sereno MI, and Dale AM (1999). Cortical surface-based analysis: II. Inflation, flattening, and a surface-based coordinate system. Neuroimage 9, 195–207. 10.1006/nimg.1998.0396. [PubMed: 9931269]

125. Soper DJ, Reich D, Ross A, Salami P, Cash SS, Basu I, Peled N, and Paulk AC (2023). Modular pipeline for reconstruction and localization of implanted intracranial ECoG and sEEG electrodes. PLoS One 18, e0287921. 10.1371/JOURNAL.PONE.0287921. [PubMed: 37418486]

126. Peled N, Gholipour T, Paulk AC, Felsenstein O, Eichenlaub JB, Dougherty DD, Widge AS, Eskandar EN, Cash SS, Hamalainen MSS,. (2017). Invasive Electrodes Identification and Labeling. GitHub Repos.

127. Dykstra AR, Chan AM, Quinn BT, Zepeda R, Keller CJ, Cormier J, Madsen JR, Eskandar EN, and Cash SS (2012). Individualized localization and cortical surface-based registration of intracranial electrodes. Neuroimage 59, 3563–3570. 10.1016/J.NEUROIMAGE.2011.11.046. [PubMed: 22155045]

128. Purdon PL, Pierce ET, Mukamel EA, Prerau MJ, Walsh JL, Wong KFK, Salazar-Gomez AF, Harrell PG, Sampson AL, Cimenser A, et al. (2013). Electroencephalogram signatures of loss and recovery of consciousness from propofol. Proc. Natl. Acad. Sci. U. S. A. 110. 10.1073/PNAS.1221180110.

129. von Ellenrieder N, Peter-Derex L, Gotman J, and Frauscher B (2022). SleepSEEG: automatic sleep scoring using intracranial EEG recordings only. J. Neural Eng. 19. 10.1088/1741-2552/AC6829.

130. Chang J-Y, Pigorini A, Massimini M, Tononi G, Nobili L, and Van Veen BD (2012). Multivariate autoregressive models with exogenous inputs for intracerebral responses to direct electrical stimulation of the human brain. Front. Hum. Neurosci. 6, 317. 10.3389/fnhum.2012.00317. [PubMed: 23226122]

131. Keller CJ, Huang Y, Herrero JL, Fini ME, Du V, Lado FA, Honey CJ, and Mehta AD (2018). Induction and Quantification of Excitability Changes in Human Cortical Networks. J. Neurosci. 38, 5384–5398. 10.1523/JNEUROSCI.1088-17.2018. [PubMed: 29875229]

132. Rubinov M, and Sporns O (2010). Complex network measures of brain connectivity: Uses and interpretations. Neuroimage 52, 1059–1069. 10.1016/J.NEUROIMAGE.2009.10.003. [PubMed: 19819337]

133. Garrett DD, Samanez-Larkin GR, MacDonald SWS, Lindenberger U, McIntosh AR, and Grady CL (2013). Moment-to-moment brain signal variability: a next frontier in human brain mapping? Neurosci. Biobehav. Rev. 37, 610–624. 10.1016/J.NEUBIOREV.2013.02.015. [PubMed: 23458776]

134. Kundu B, Davis TS, Philip B, Smith EH, Arain A, Peters A, Newman B, Butson CR, and Rolston JD (2020). A systematic exploration of parameters affecting evoked intracranial potentials in patients with epilepsy. Brain Stimul. 13, 1232–1244. 10.1016/J.BRS.2020.06.002. [PubMed: 32504827]

135. Dionisio S, Mayoglou L, Cho SM, Prime D, Flanigan PM, Lega B, Mosher J, Leahy R, Gonzalez-Martinez J, and Nair D (2019). Connectivity of the human insula: A cortico-cortical evoked potential (CCEP) study. Cortex. 120, 419–442. 10.1016/J.CORTEX.2019.05.019. [PubMed: 31442863]

Highlights

- Decreased complexity and connectivity, with increased variability when unconscious.
- Changes were more pronounced during propofol-induced general anesthesia than sleep.
- During sleep, changes were homogeneously distributed across the human brain.
- During anesthesia substantial prefrontal disconnection related to lack of arousability.

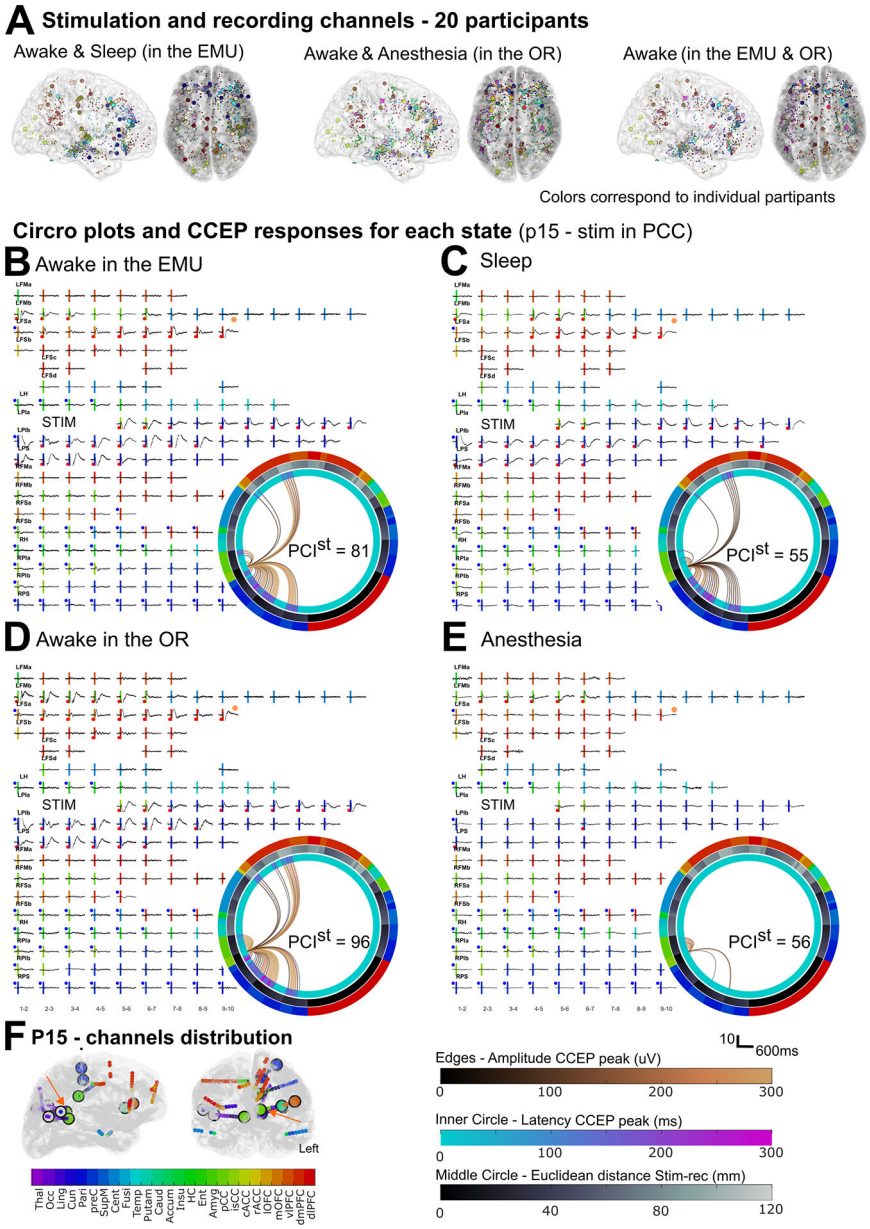

Figure 1. CCEP response to stimulation in different brain states.

(A) Distribution of stimulation (circles) and recording (dots) channels across the N = 20 participants grouped by awake and sleep in the EMU (N = 13; s = 99 stimulation channels; r = 1547 recording channels), and awake and propofol-induced general anesthesia before electrode explantation in the OR (N = 14, s = 3635, r = 1709), and awake in the EMU and the OR (N = 13, s = 34, r = 1479). B-E) CCEP responses in a representative participant (p15) while awake (B) and during natural sleep (C); while awake (D) and under anesthesia (E). Vertical line: stimulation time, with color denoting anatomical location; orange dot: example in Fig. 2.b. Inset (B-E): Circro plots with edges as connections from stimulation to recording channels. Edge color: amplitude of the most prominent peak (hot colormap); inner circle: latency of the first peak (winter colormap); middle circle: Euclidean distance between recording and stimulation channel (bone colormap); outer ring: anatomical location. Left

(right) half corresponds to channels in the left (right) hemisphere. F) Channels distribution for this participant. Orange arrows: stimulation channel in B-E. See also Fig. S1 and Table S1.

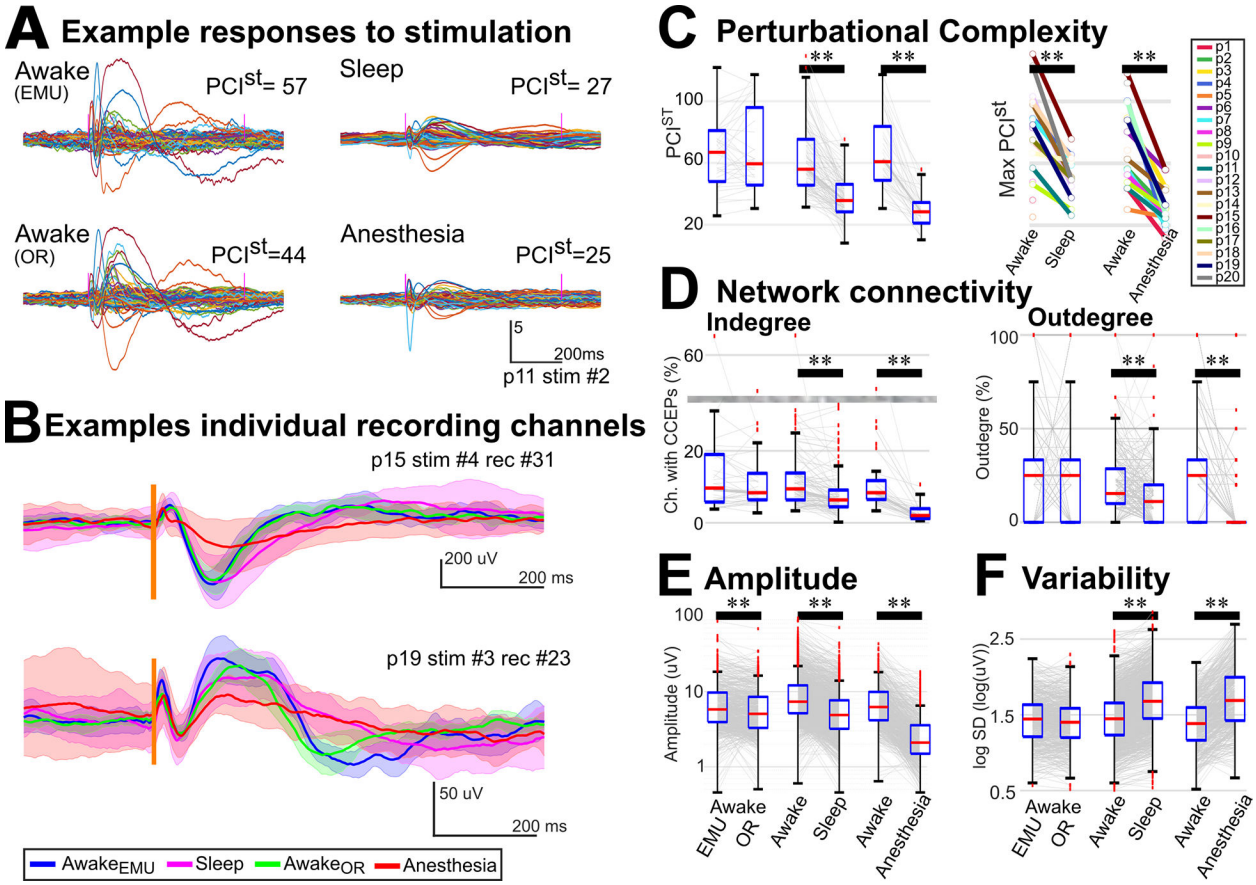

Figure 2. Complexity, CCEP Connectivity, CCEP features, and Variability during different states.

A) Representative example of z-scored averaged intracranial EEG following stimulation cortex (p11; stimulation in PFC). This illustrates reduced perturbational complexity (PCI^{st}) during unconscious states (sleep & anesthesia). Colored lines: individual recording channels. B) Representative examples of variability across states in two recording channels (p15 & p19). Mean and standard deviation of the intracranial EEG during awake in the EMU (blue trace), sleep (magenta), awake in the OR (green), and anesthesia (red). Spread was large for anesthesia, corresponding to large inter-trial variability. Vertical line: stimulation time. C) *Left*: Complexity was reduced during sleep compared to awake (N=13, s=99) and during anesthesia compared to awake (N=14, s=36) in the same environment. *Right*: Maximum complexity was reduced for each participant during unconscious states. (D) CCEP indegree (left) and outdegree (right) connectivity were reduced during sleep (N = 13, s = 99, r = 860) and anesthesia compared with awake (N = 14, s = 36, r = 562). Grayed area indicates a cut in the scale. (E) The response amplitude was reduced during sleep (r = 1527) and anesthesia (r=573) compared to awake. Notably during anesthesia, the amplitude was reduced in almost all channels while during sleep, even though for most channels it was reduced (A and Fig. 1.C), in some it was similar (B) or even larger (Fig. S3) during sleep than awake. (F) Inter-stimulation variability increased during sleep (r = 1527) and anesthesia (r=573) compared to awake. C&D: Wilcoxon tests; E&F: permutation tests. ** indicates $p<0.01$. Gray lines: individual stimulation (C&D) or recording (E&F) channels.

CCEP: cortico-cortical evoked potential; N: number of participants; s: number of stimulation channels; r: number of recording channels. See also Fig. S3 and Tables S2 & S3.

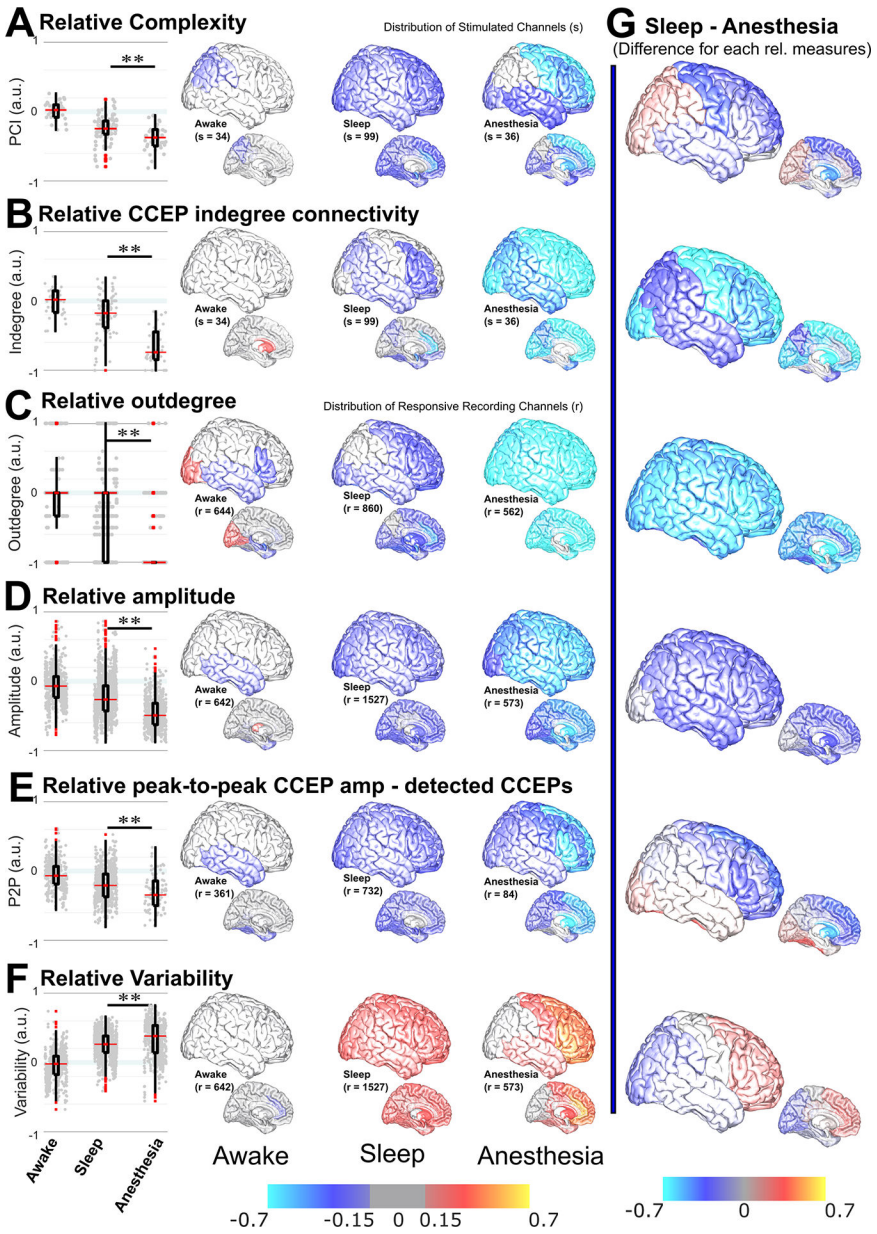

Figure 3. Relative measures comparing sleep vs. anesthesia.

Relative measures allowed comparison of arousable (sleep) vs. unarousable (anesthesia) unconscious states. *Left*: Positive (negative) values, bounded at +1 (−1), corresponded to an increase (decrease) in the relative measure. A *wake* corresponded to awake in the OR normalized by awake in the EMU, *sleep* was normalized by awake in the EMU, and *anesthesia* was normalized by awake in the OR. All relative measures were statistically different for sleep vs. anesthesia. Relative (A) complexity, (B) CCEP indegree connectivity, (C) outdegree, (D) amplitude across recording channels, and (E) peak-to-peak amplitude of the detected CCEPs (P2P), were significantly smaller for anesthesia than for sleep; F) Variability was significantly larger. *Middle*: Anatomical distribution of the averaged relative measure within a region pooling together participants and channels and plotted in the Collin27 atlas brain (*left*: awake; *middle*: sleep; *right*: anesthesia). *Top row*: lateral cortical

regions (right and left hemispheres were merged); *bottom row*: subcortical and mesial regions. A) The anatomical distribution of relative complexity showed almost no changes during awake states, a uniform decrease across the brain during sleep, and a predominant decrease in frontal regions during anesthesia. B) The distribution of indegree showed almost no changes during awake states, while a decrease in parts of the brain was observed during sleep. During anesthesia, the relative CCEP connectivity decreased across the brain, with the most negative values in the frontal and occipital regions. C) For outdegree, frontal, central, occipital, and subcortical regions decreased during sleep, but the dispersion was large. During anesthesia, outdegree profoundly decreased across the brain, median = −1. D) Relative amplitude decreased across the brain during sleep, while during anesthesia it was more pronounced in anterior than posterior regions. E) Even when in some regions there was no difference in connectivity, the relative peak-to-peak amplitude of those CCEP responses homogenously decreased across the brain during sleep. Relative peak-to-peak CCEP amplitude during anesthesia decreased across the brain, with more negative values in prefrontal regions than anywhere else. F) The anatomical distribution of relative variability showed a uniform increase across the brain during sleep, and an increase in frontal and temporal regions, with larger values in prefrontal regions, during anesthesia. For awake in different environments, there were only a few differences, predominantly a decrease in the temporal lobe in the OR for outdegree and amplitude measures. G) Regional difference between sleep and anesthesia. A clear picture of the regional differences between sleep and anesthesia was obtained by subtracting the mean value per region for sleep minus anesthesia for each relative measure. There was an overall reduction of connectivity and amplitude for anesthesia. The prefrontal regions showed overall more pronounced changes, with decreased complexity, connectivity, and CCEP amplitude. Variability was larger in the prefrontal cortex for anesthesia minus sleep and smaller in posterior regions. Stimulation channels were considered for complexity and indegree and recording channels for the other measures. Gray dots in boxplots indicate individual stimulation (in A & B) or recording (in D-F) channels. In the distribution of relative measures, Red/orange/yellow indicated an increase while blue/cyan indicated a decrease. In the central figures, a threshold was set at |0.15|, with values −0.15 to +0.15 in gray. Mann–Whitney U-test was used for complexity, indegree, and outdegree. LMM & permutation tests were used for amplitude and variability. ** $p<0.01$. s: number of stimulated channels; r: number of recording channels. For relative values at individual stimulation channels, see Figure S4. See also Tables S4 & S5.

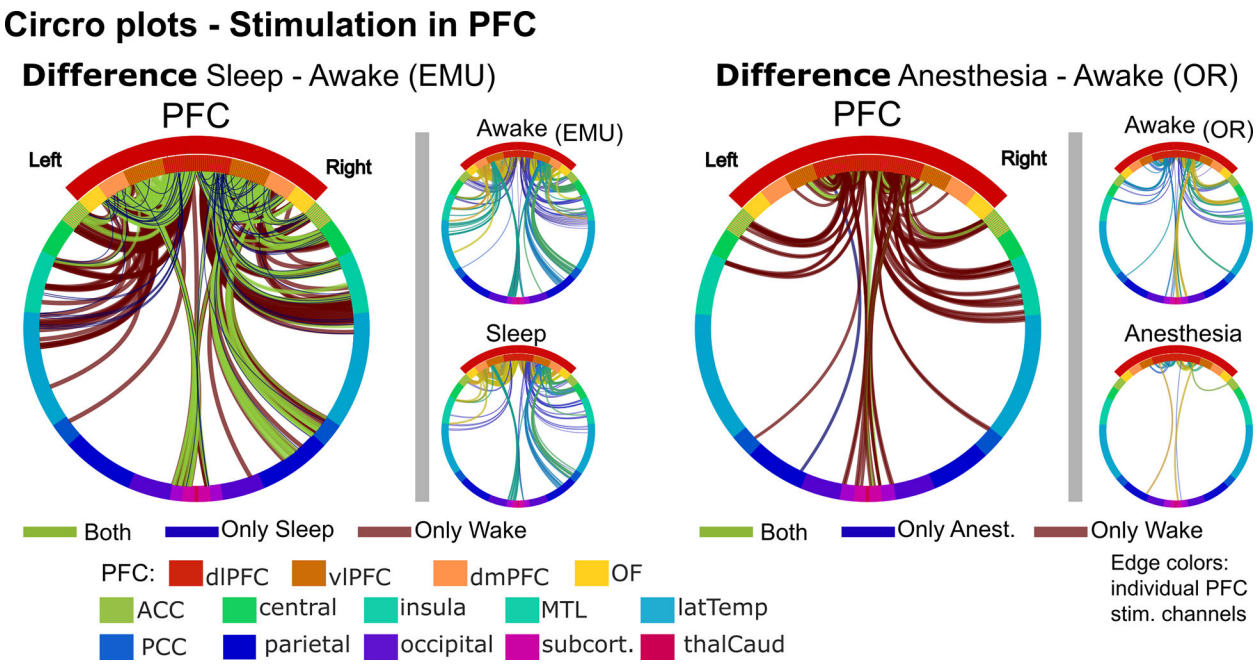

Figure 4. Circro plots of the difference in connections per state for PFC stimulation.

Circro plots for PFC stimulation regions comparing sleep vs. awake in the EMU (left) and anesthesia vs. awake in the OR (right). Large d*ifference* Circro plots illustrate the connections that were only present during wake (red), only during the unconscious state (blue), or that did not change (green). Smaller Circro plots correspond to each stimulation channel in the PFC. Edges represent connected channels colored by stimulation channel. Ring colors: anatomical region. Regions encompassing the PFC are within the red arc. Left (right) half of Circro plots correspond to the left (right) hemisphere.

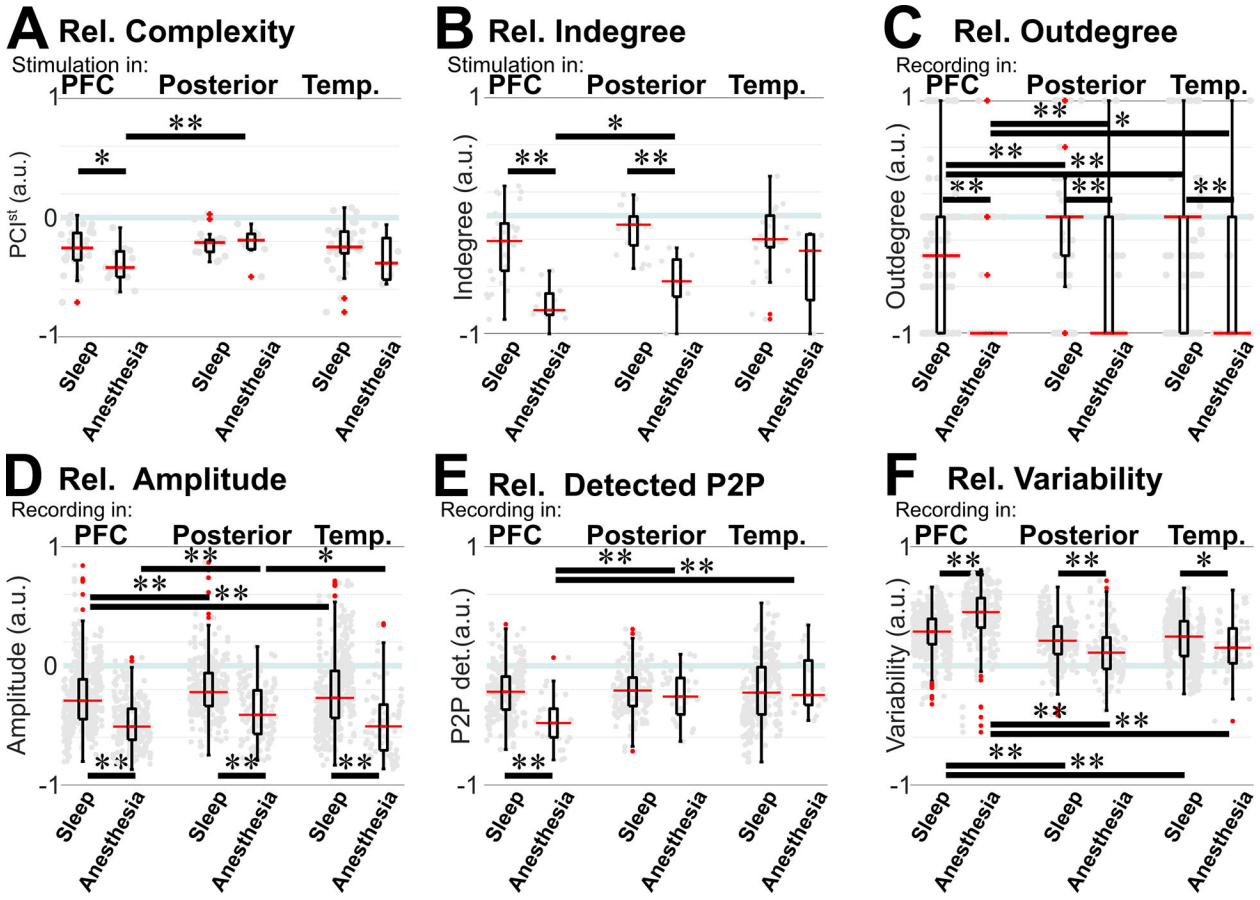

Figure 5. Comparison of relative measures during sleep vs. anesthesia and between regions.

A) Relative complexity was smaller for anesthesia than sleep with stimulation in the PFC, but similar with posterior stimulation. Within anesthesia, it was smaller for PFC than posterior stimulation; no significant difference was found between regions for sleep. B) Relative indegree was smaller for anesthesia than sleep with PFC or posterior stimulation. Within anesthesia, it was smaller for PFC than posterior stimulation; no significant difference was found between regions for sleep. C) Relative outdegree connectivity was smaller for anesthesia than for sleep regardless of recording region. Within anesthesia and within sleep, it was smaller for PFC than posterior or temporal channels. D) Relative amplitude was smaller for anesthesia than for sleep regardless of recording region. Within anesthesia and within sleep, it was smaller for PFC than posterior channels. E) Relative peak-to-peak amplitude of the detected CCEPs was smaller for anesthesia than sleep for PFC but not for posterior or temporal CCEP responses. Within anesthesia, it was smaller for PFC than posterior or temporal channels; no significant difference was found between regions for sleep. F) Relative variability was larger for anesthesia than sleep for PFC recordings. Interestingly, the opposite occurred for posterior or temporal recordings, where variability was smaller during anesthesia than during sleep. Within anesthesia and within sleep, variability was smaller for PFC than posterior or temporal channels. Gray dots: individual stimulation or recording channels. A-C: Mann–Whitney U-Mann test; D-F: permutation test. ** $p<0.01$; * $0.01 \geq p > 0.05$. PFC: prefrontal cortex; P2P: peak-to-peak

CCEP amplitude; s: number of stimulated channels; r: number of recording channels with stimulation anywhere. See also Table S4–S6.

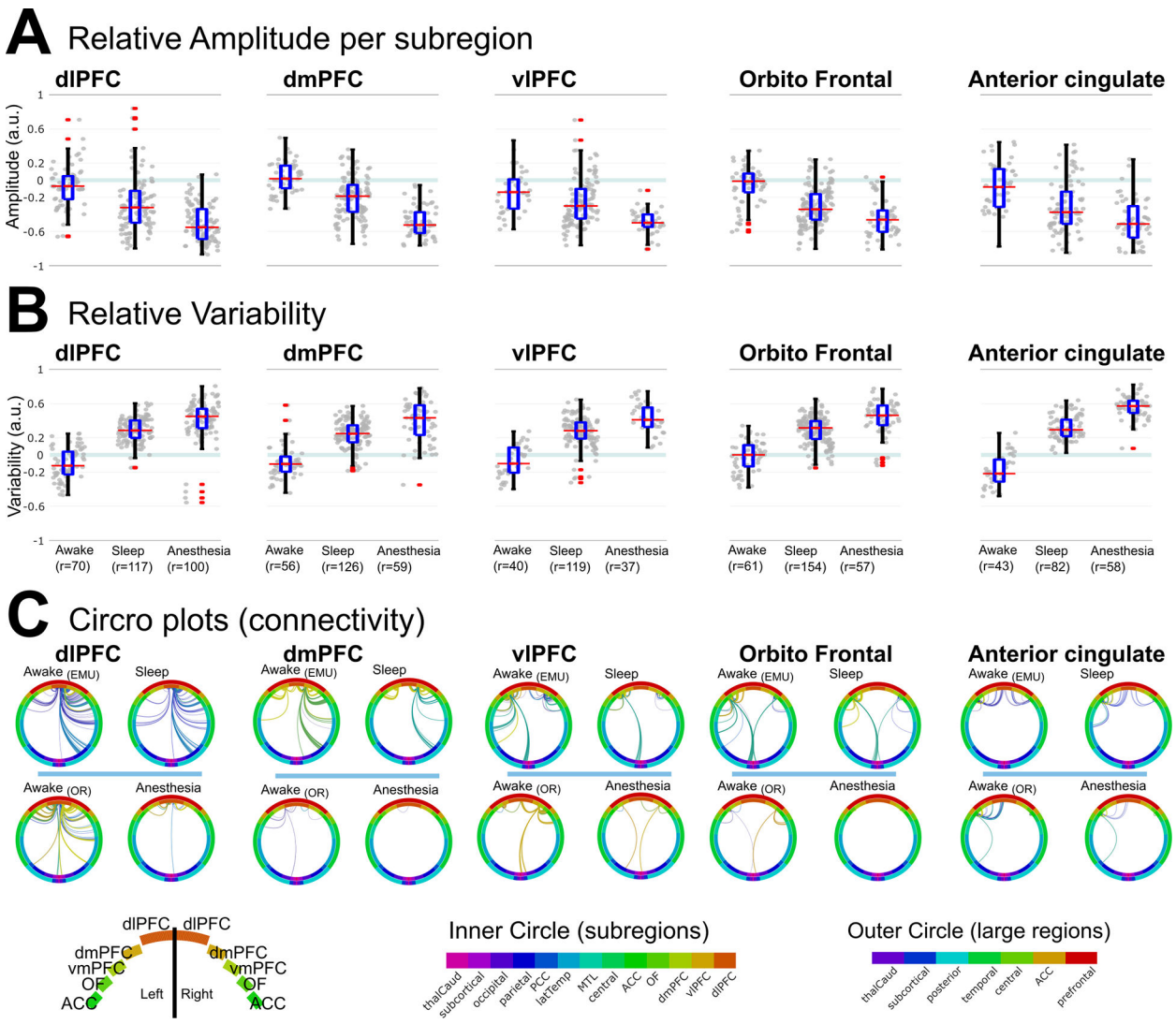

Figure 6. Relative measures for subregions of the prefrontal cortex showed consistent changes.

A) Relative amplitude was smaller for anesthesia than sleep for each of the subregions of the PFC and for the anterior cingulate. B) Relative Variability was larger for anesthesia than sleep for each of the subregions of the PFC and for the anterior cingulate. C) Circos plots of connections in each state. *Top*: during awake and sleep in the EMU, some connections were preserved. *Bottom*: during anesthesia, most connections disappeared. Edge colors: individual stimulation channels; *inner ring*: subregions; *outer ring*: lobes; *PFC*: prefrontal cortex; *dlPFC*: dorsolateral PFC; *dmPFC*: dorsomedial PFC; *vlPFC*: ventrolateral PFC. See also Table S5.

REAGENT or RESOURCE	SOURCE	IDENTIFIER
Deposited data		
De-identified human/patient standardized data	This paper	https://dabi.loni.usc.edu/dsi/9XQD2CWZG484
Software and algorithms		
CCEPLOC - analysis and visualization code created for this paper (https://github.com/Center-For-Neurotechnology/CCEPLOC)	This paper	DOI: 10.5281/zenodo.8211944
CereLAB (https://github.com/Center-For-Neurotechnology/CereLAB)	This paper	DOI: 10.5281/zenodo.8211952
FreeSurfer	Dale et al[123]; Fischl et al.[124]	RRID:SCR_001847
MATLAB	MathWorks	RRID:SCR_001622
Permutation test for MATLAB	Krol	https://github.com/lrkrol/permutationTest
Circro	Bonilha; Dionisio et al.[135]	https://github.com/bonilhamusclab/circro
MMVT	Peled	DOI: 10.5281/zenodo.438343